Radioactive decay — ^{14}C dating

Radiometric dating — by far the best way to determine the ages of rocks, meteorites, archaeological sites.

In addition to the stable isotopes (Fig 2-2) there are many that are unstable

Example ^{14}C — the heaviest naturally occurring isotope of carbon

Decays to ^{14}N by β decay

$$^{14}C \rightarrow {}^{14}N + e^-$$

$Z = 6$ $\quad$ $Z = 7$

Radioactive decay — in general

Example : 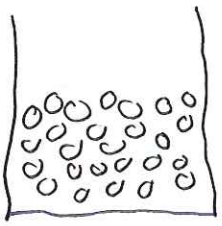 radioactive atoms in a jar

Each atom has an equal probability of decay. Probability that a randomly selected atom will decay in an infinitesimal time interval

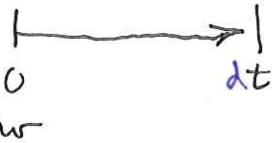

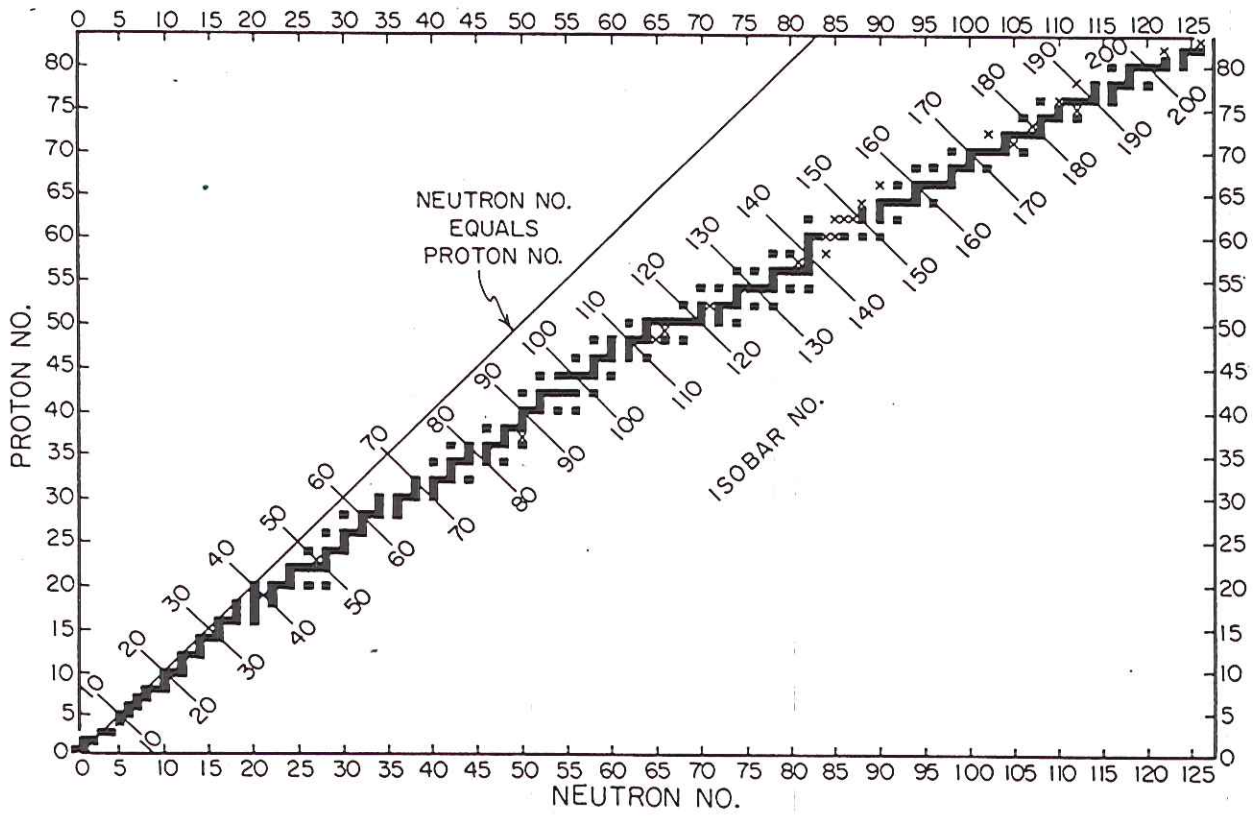

Figure 2-2. Stable nuclide configurations: The squares represent stable combinations of neutrons and protons. The x's represent radioactive nuclides whose half-lives are so long that they survive billions of years after their formation in stars. All the remaining combinations are radioactive with half-lives sufficiently short that they are no longer present in the solar system. Nuclides lying along the same horizontal line (i.e., those with the same proton number) are referred to as isotopes. Those falling along the same vertical line (i.e., those with the same number of neutrons) are referred to as isotones. Those falling along the same diagonal line (i.e., those with the same number of nuclear particles) are called isobars. The diagram terminates with the heaviest stable nuclide (^{209}Bi).

P(decay in time dt) = $p\,(dt)$

p = probability of decay / unit time

Say there are 10^6 atoms in jar at $t = 0$

$N_0 = 10^6 = 1{,}000{,}000$

At $t = 1$ yr there will be

say $p = 0.01$

$N_1 = 10^6 (1-p) = 990{,}000$

p is the percent that decay per year
Our unit time is 1 year

$$p = \frac{\text{percent that decay}}{\text{unit time}}$$

in our case 1% decay every year

At $t = 2$ yr, $N_2 = 990{,}000\,(1-p)$

$= 10^6 (1-p)^2 = 980{,}100$

At $t = 100$ yr

$N_{100} = 10^6 (1-p)^{100} = 366{,}032$

The general formula is $N_t = N_0 (1-p)^t$

N_t ↑ # remaining at time t

Recall that $a^t = e^{t \ln a}$

$$N_t = N_0 e^{t \ln(1-p)}$$

Define the decay constant

$$\boxed{\lambda = -\ln(1-p)}$$ ← this will be > 0

Then $$\boxed{N_t = N_0 e^{-\lambda t}}$$ ← exponential decay

For small p, $\lambda \approx p$

For example $-\ln(1-0.01) = 0.01005$

Change notation:

P_t = # parent atoms

D_t = # daughter atoms

↑ why not son or offspring? (I don't know)

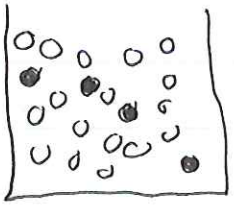

○ parent

● daughter

See Fig. 3.2

Then $$\boxed{\begin{aligned} P_t &= P_0 e^{-\lambda t} \\ D_t &= P_0 - P_t = P_0(1-e^{-\lambda t}) \end{aligned}}$$

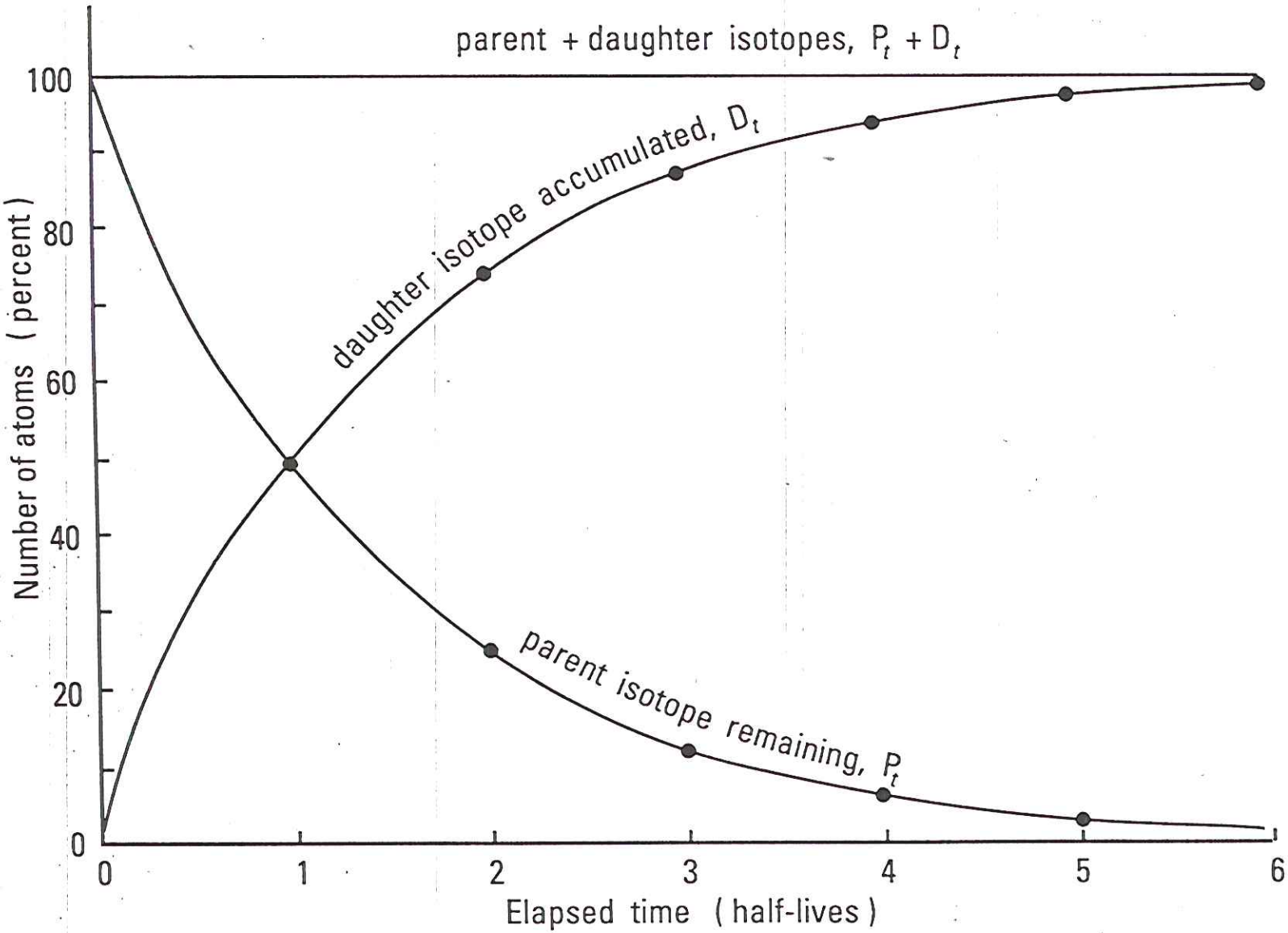

Fig. 3.2. Decay of a radioactive parent isotope and the corresponding accumulation of its daughter isotope. In a closed system, the sum of the parent and daughter isotopes at any time equals the original amount of the parent isotope.

Note that time expressed in half-lives

Amount of time elapsed when

$$P_t = \frac{1}{2} P_0 \quad , \quad D_t = \frac{1}{2} P_0$$

$$\frac{1}{2} P_0 = P_0 \, e^{-\lambda \tau_{1/2}}$$

$$\lambda \tau_{1/2} = -\ln\left(\frac{1}{2}\right) = \ln 2$$

$$\boxed{\tau_{1/2} = \frac{\ln 2}{\lambda} = \frac{0.693}{\lambda}}$$

Note that after two half lives

$$P_t = \frac{1}{4} P_0 \quad , \quad D_t = \frac{3}{4} P_0$$

At all times $P_t + D_t = P_0$

The fraction remaining after n half lives is

$$\boxed{\text{fraction after } n \text{ half lives} = \left(\frac{1}{2}\right)^n}$$

After 10 half lives only $\frac{1}{1024}$ remaining

It is difficult to measure concentrations that are too low — for this reason it is difficult to date samples older than ~ 10 half lives

Age determination : $P_t = P_0 e^{-\lambda t}$

$$\lambda t = -\ln (P_t/P_0)$$

$$\boxed{t = \frac{1}{\lambda} \ln \left(\frac{P_0}{P_t} \right)}$$

knowledge of amount of parent at time zero required

This equation works for ^{14}C but usually don't know P_0. What then?

$$P_t = P_0 e^{-\lambda t} \Rightarrow P_0 = P_t e^{\lambda t}$$

$$D_t = P_0 (1 - e^{-\lambda t}) = P_t e^{\lambda t} (1 - e^{-\lambda t})$$

$$= P_t (e^{\lambda t} - 1)$$

$$e^{\lambda t} = \frac{D_t}{P_t} + 1$$

$$\boxed{t = \frac{1}{\lambda} \ln \left(\frac{D_t}{P_t} + 1 \right)}$$

in terms of amounts P_t, D_t of parent & daughter now

The above is for the simple case that $D_0 = 0$.

There may, however, have been black balls in the jar to begin with

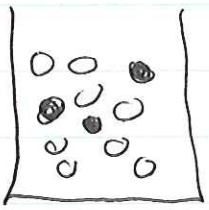

• daughter D_0

$t = 0$

Then $$D_t = D_0 + P_0 (1 - e^{-\lambda t})$$

$$= D_0 + P_t (e^{\lambda t} - 1)$$

$$\boxed{t = \frac{1}{\lambda} \ln \left(\frac{D_t - D_0}{P_t} + 1 \right)}$$

Must correct for the initial amount of the daughter by subtraction.

Actually three methods

- P_0 known (e.g. ^{14}C)

Three ~~Two~~ methods used in practice:

- D_0 negligible — K-Ar
- D_0 ~~not needed~~ determined from t=now measurements — isochron method

^{14}C dating: not used to date rocks or meteorites but many important applications

Carbon has 3 principal isotopes

^{12}C — 99%
^{13}C — 1%
^{14}C — unstable, $\tau_{1/2} = 5730 \pm 30$ yrs

β decay — see figure

Question — if $\oplus$ is 4.5 b.y. old how can there be any ^{14}C?

Answer: it is constantly being produced in the stratosphere (above 15 km) by neutron capture

Cosmic ray → fast neutrons

$$n + {}^{14}N \rightarrow {}^{14}C + p^+ + e^-$$

See Fig. 5.2 Lunine

$^{14}N_2$ is main constituent of atmosphere

N_2 — 80% of atmosphere

^{14}N 99.6%
^{15}N 0.4%

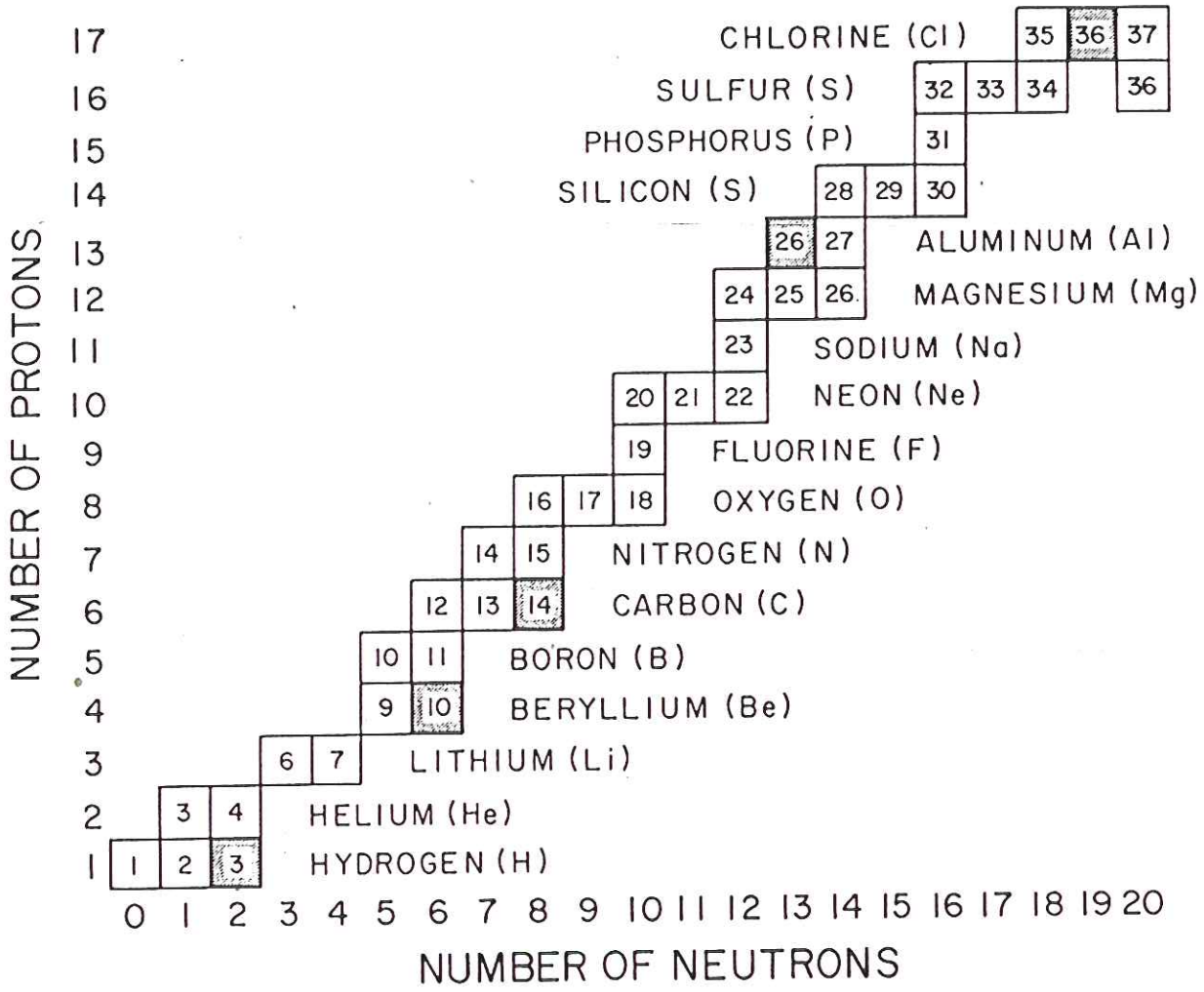

BETA DECAY

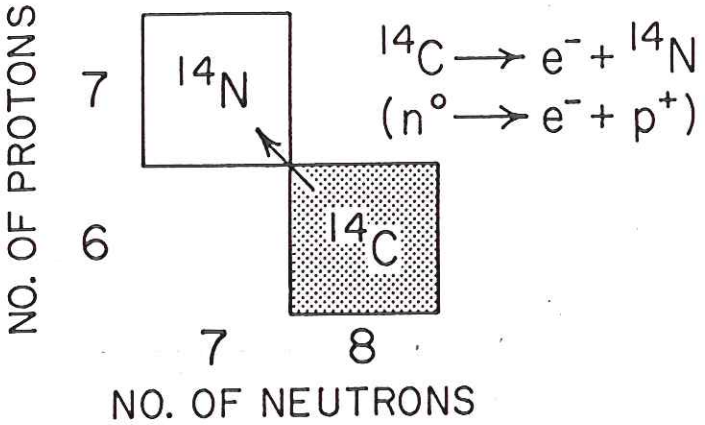

Half life of ^{14}C

5730 ± 30 years

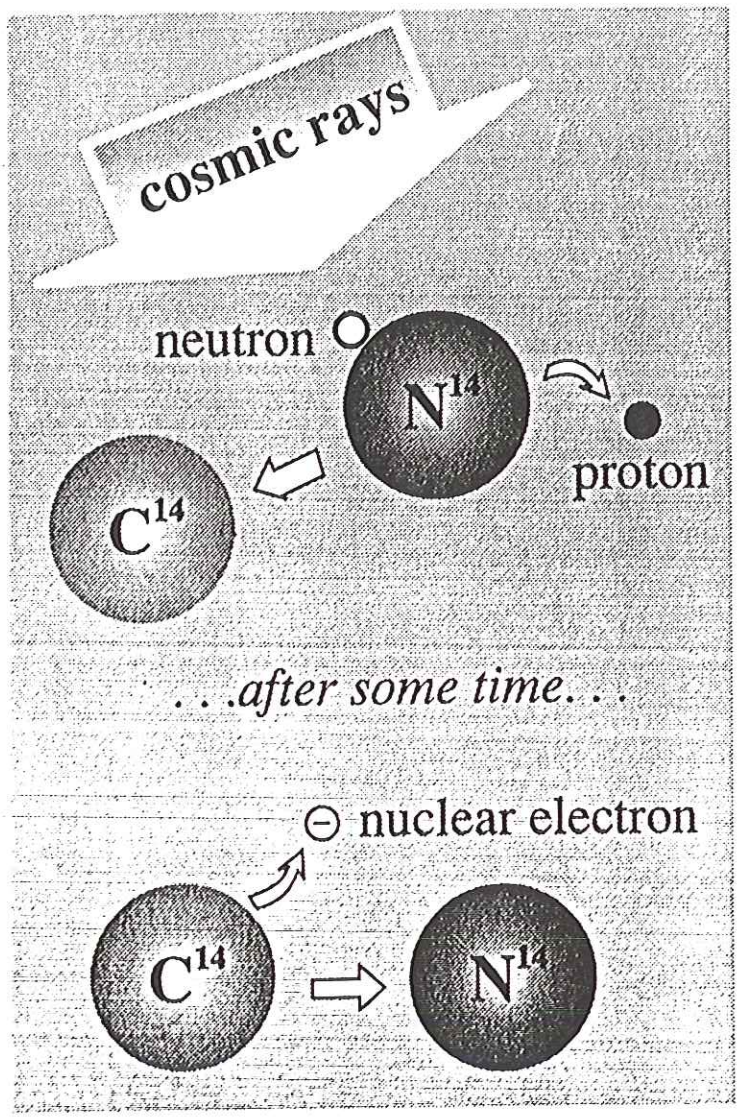

Figure 5.2. Production of ^{14}C from nitrogen and cosmic rays, and its decay. After Cloud (1988, p. 84).

The amount of ^{14}C in the atmosphere depends upon the efficiency of $^{14}N \rightarrow {}^{14}C$ production.

Initially assumed steady state:

Let C be the cosmic ray production rate (new ^{14}C atoms / year)

Then

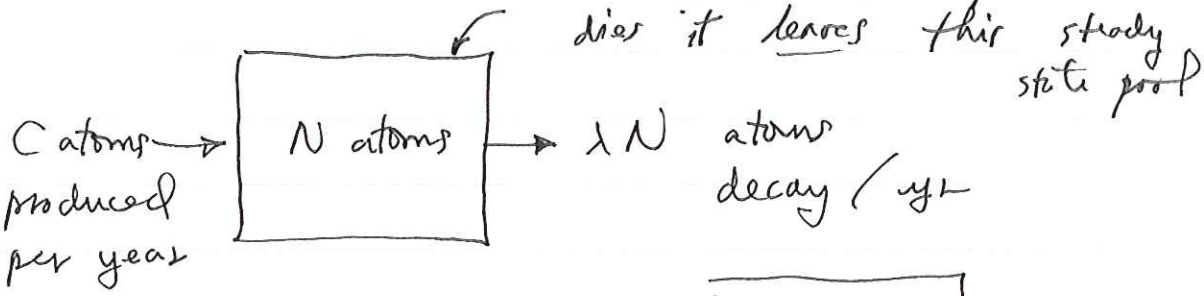

$$C = \lambda N \quad \text{or} \quad \boxed{N = \frac{C}{\lambda}}$$

As we shall see, C in fact varies slowly with time,

$$\boxed{N_t = \frac{C_t}{\lambda}}$$

The ^{14}C in the atmosphere is present in CO_2

Ratio of $\left(\frac{^{14}C}{^{12}C}\right)_{atm} \approx 10^{-12}$

M. Bender

Figure 7.15 J&R shows how ^{14}C dating is done.

All living things share $\left(\frac{^{14}C}{^{12}C}\right)_{atm}$

Plants are made from atmospheric CO_2 by photosynthesis

$$CO_2 + H_2O \rightarrow \underbrace{CH_2O}_{\text{plant carbohydrate}} + O_2$$

Animals eat plants

$$\left(^{14}C\right)_{\text{dead organic matter}} = \left(^{14}C\right)_{atm} e^{-\lambda t}$$

$$\lambda = \frac{0.693}{5730 \text{ yrs}} = 1.21 \cdot 10^{-4} \text{ yr}^{-1}$$

Divide by $\left(^{12}C\right)_{atm} = \left(^{12}C\right)_{\text{dead matter}}$

$$\left(\frac{^{14}C}{^{12}C}\right)_{sample} = \left(\frac{^{14}C}{^{12}C}\right)_{atmos} e^{-\lambda t}$$

$$t = \frac{1}{\lambda} \ln \frac{\left(^{14}C/^{12}C\right)_{atmos}}{\left(^{14}C/^{12}C\right)_{sample}}$$

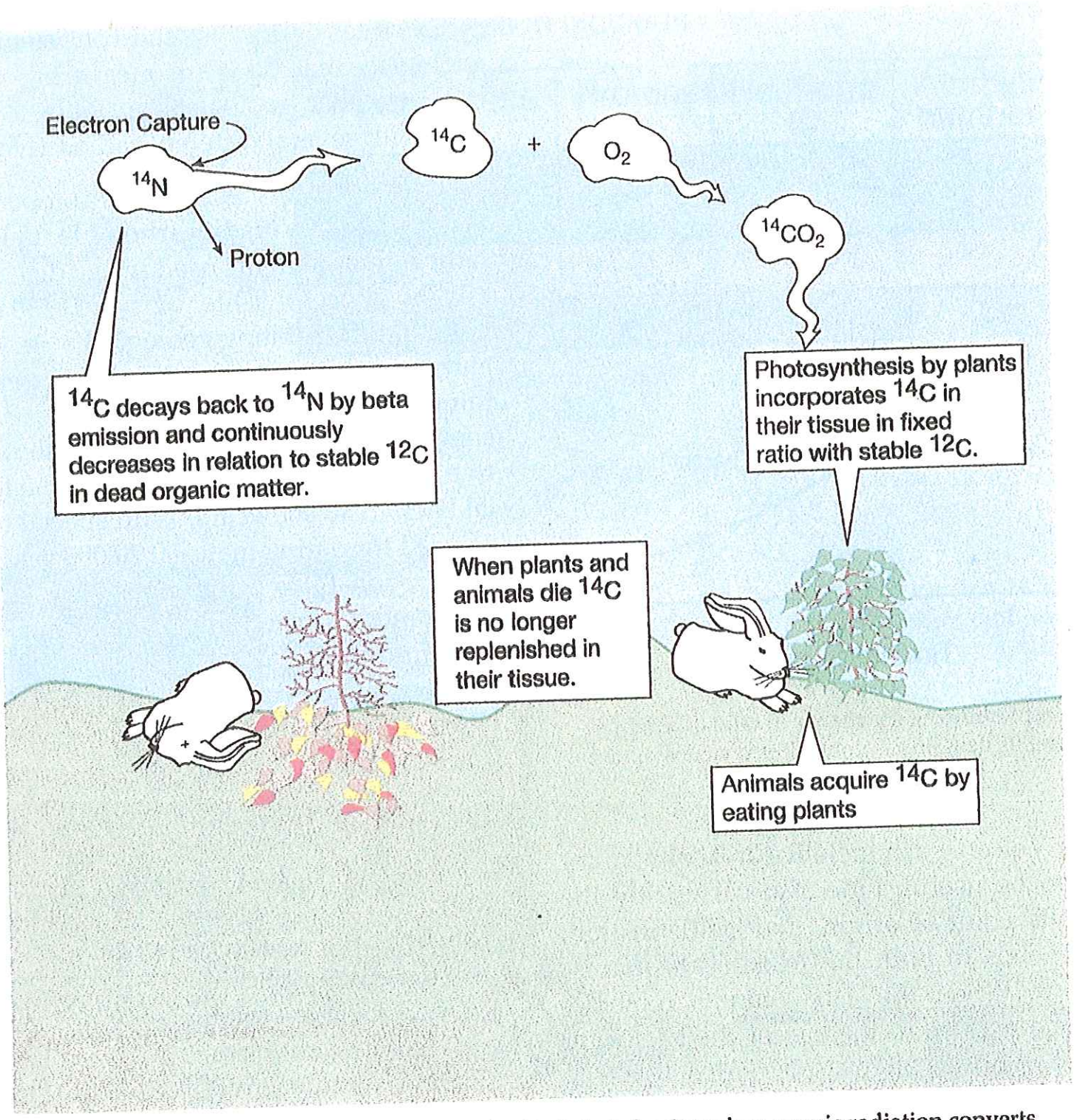

FIGURE 7.15 The path of radiocarbon in the food chain begins when cosmic radiation converts ^{14}N to ^{14}C in the atmosphere. The radiocarbon then combines with atmospheric oxygen to form $^{14}CO_2$ (carbon dioxide) in a constant ratio with the carbon dioxide of stable carbon, ^{12}C and ^{13}C. Photosynthesis by plants uses this $^{14}CO_2$, water, and solar energy and thus brings radiocarbon into the plant tissue. As long as the plant lives there is a constant ratio between the radiocarbon and the stable forms of carbon, ^{12}C and ^{13}C, in their tissue. Animals acquire radiocarbon by eating plants, or eating animals who have fed on plants. When the plants and animals die their supply of radiocarbon is no longer replenished. As it decays back to ^{14}N, less and less ^{14}C remains in the plant and animal, but the amount of stable carbon does not change. As a result, the ratio between ^{14}C and stable carbon

Method developed by Willard Libby
- Received the Nobel Prize for this work — later got involved with Nobel Prize speaker bank!

He measured $^{14}C_{atmos}$ & $^{14}C_{sample}$ using a geiger counter to detect the e^- emitted during the decay.

Many disadvantages

- in old samples P_t/P_0 is small — requires large amounts of sample and/or very long counting times

Show Libby's 1955 demonstration that the dates were reliable

Compared to known dates in historical record, as well as to tree rings — see Fig. 2.1

Oldest dates Egyptian ~ 3000 BC
Dated by Egyptologists (insert page 10½)

Modern method — mass spectrometry

Developed first for other isotopes

Libby's calibration curve

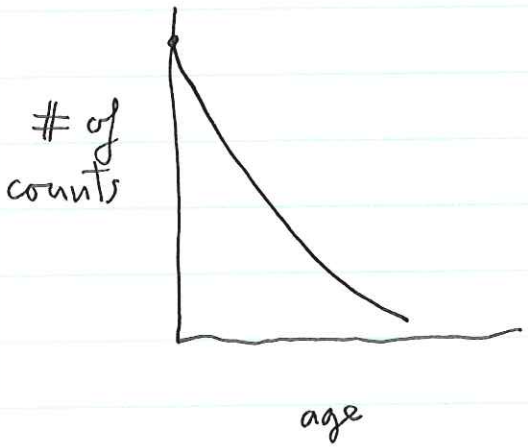

The number of decays in time dt is

$$\#\text{ decays in time } dt = \lambda P_0 e^{-\lambda t} dt = \lambda P_t dt$$

↑ proportional to amount of parent (^{14}C) remaining

Thus the curve

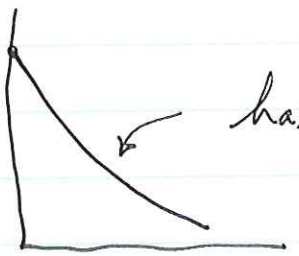

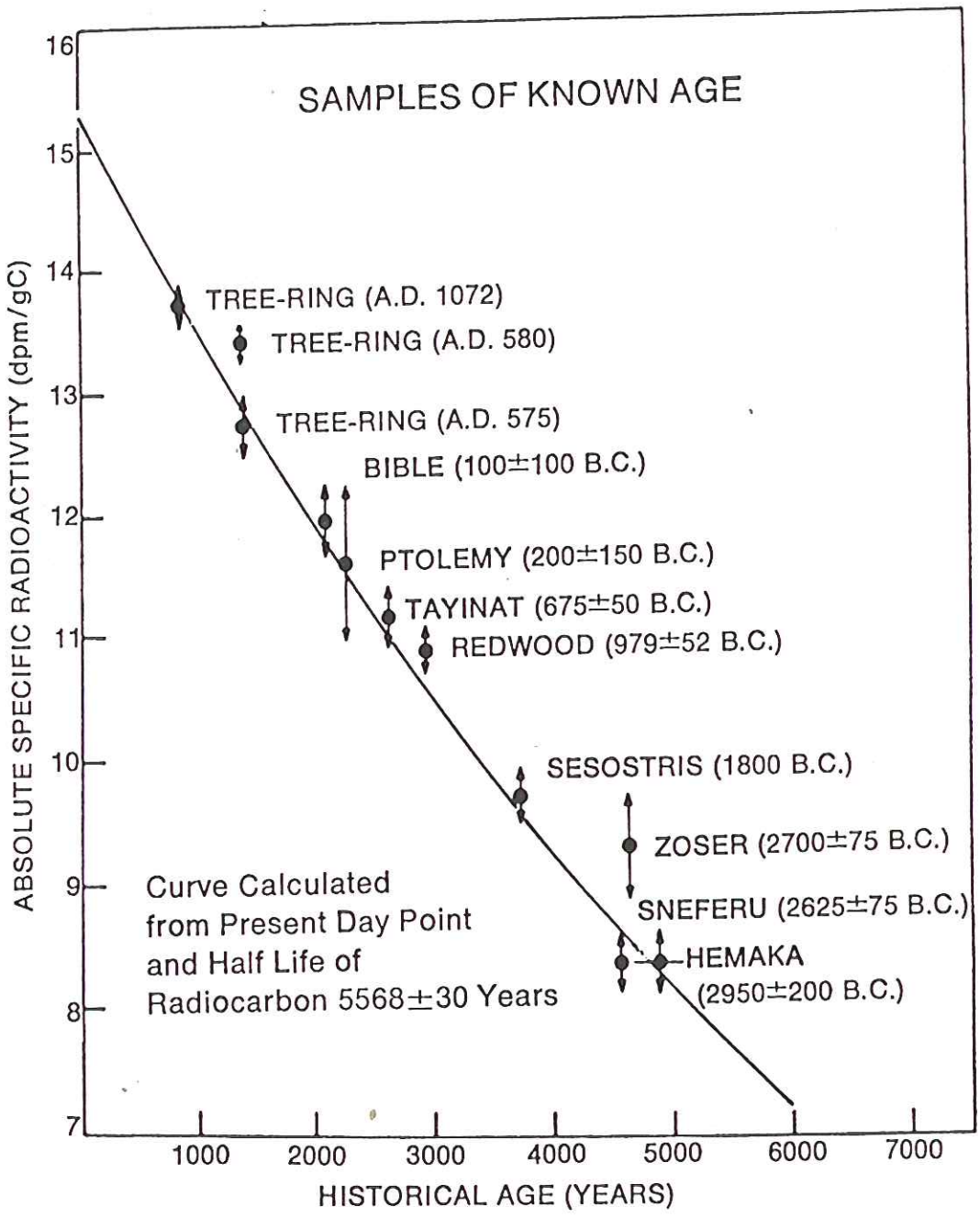

note – this axis is in counts

FIG. 10. Willard Libby's check of the basic soundness of the radiocarbon method. Observed radioactivities of historically dated samples are plotted against the curve, which shows the predicted values. The good agreement was confirmation of the validity of the method. (*After W. F. Libby*)

Younger specimens are more radioactive

$P_t = P_0 e^{-\lambda t}$

More ^{14}C in sample
⇒ more decays

FIGURE 2–1 A cross section of the trunk of a Douglas fir shows the method of dating tree rings *(dendrochronology)*. The annual variability of ring widths in this species provides a record of climate change during the life of the tree. (Photograph courtesy of the Laboratory of Tree-Ring Research, the University of Arizona.)

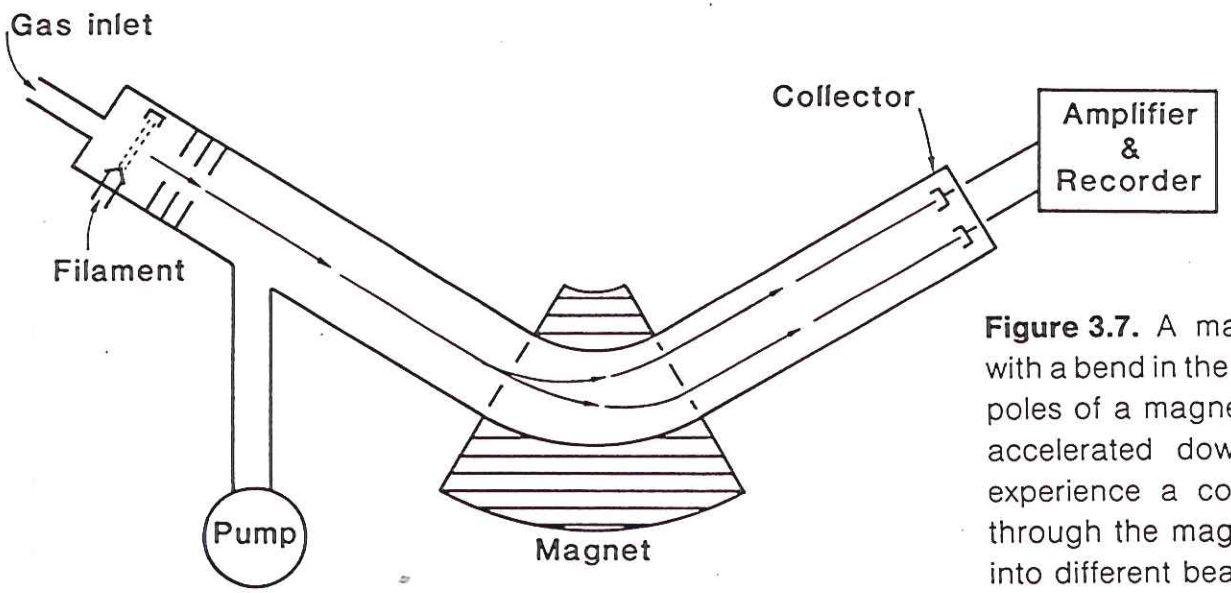

Figure 3.7. A mass spectrometer is a tube with a bend in the middle between the opposite poles of a magnet. Atomic or molecular ions accelerated downtube by a voltage drop experience a constant force while passing through the magnet and are thus separated into different beams according to mass.

lighter masses are bent more

Provides a very accurate measure of isotope ratios

Actually hard to do for ^{14}C since

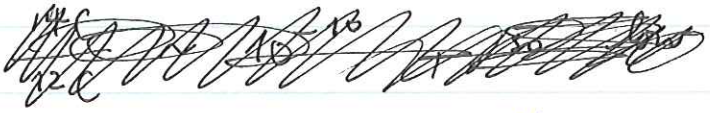

$\frac{^{14}C}{^{12}C} \approx 10^{-12}$ to 10^{-14} — very low

10^{-12}: atmosphere; 10^{-14}: sample

AMS spectrometry — arrangement more complicated than Fig. 3.7 but idea the same.

One thing used — a rotating paddle which blocks most of the ^{12}C — also a fancy detector for ^{14}C — not just a Faraday cup, which measures current.

Subsequent to Libby's pioneering work it was recognized that the ratio

$$\left(\frac{^{14}C}{^{12}C}\right)_{atm}$$

was not constant in time

C_t varies because of variations in cosmic ray flux

$$C_t \rightarrow \boxed{N_t} \rightarrow \lambda N_t$$

$$N_t \approx \frac{C_t}{\lambda}$$

Need to convert ^{14}C radiocarbon years to calendar years.

This done back to ~4000 years using bristlecone pines — Earth's oldest living inhabitants

Fig. 5.3 (Lunine) shows ^{14}C calibration back to 22,000 yr BP.

Based on U-disequilibrium dating of Barbados corals

Note that in general ^{14}C years are biased low.

This ⇒ ^{14}C production was typically higher in past

Thus, e.g., 12,000 ^{14}C yr → 14,000 yr

Minze Stuiver curve shows very accurate calibration back last 1000 yrs. For applications in which very precise dates are required

Note, however, the unavoidable ambiguity

600 ^{14}C yr BP ≈ 1330 – 1390

60 yr uncertainty

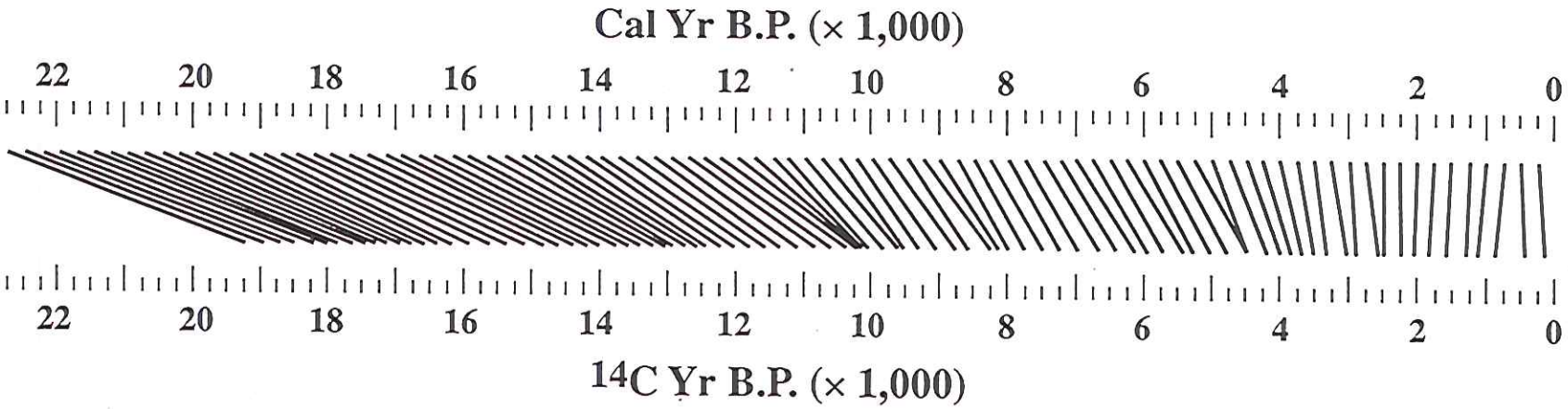

Figure 5.3. Relationship between actual age of a sample (cal yr before present; B.P.) and the age from carbon-14 dating (^{14}C yr B.P.). Both axes are in units of thousands of years, and so, the figure goes back to 22,000 years ago. From Bartlein et al. (1995) by permission of Academic Press.

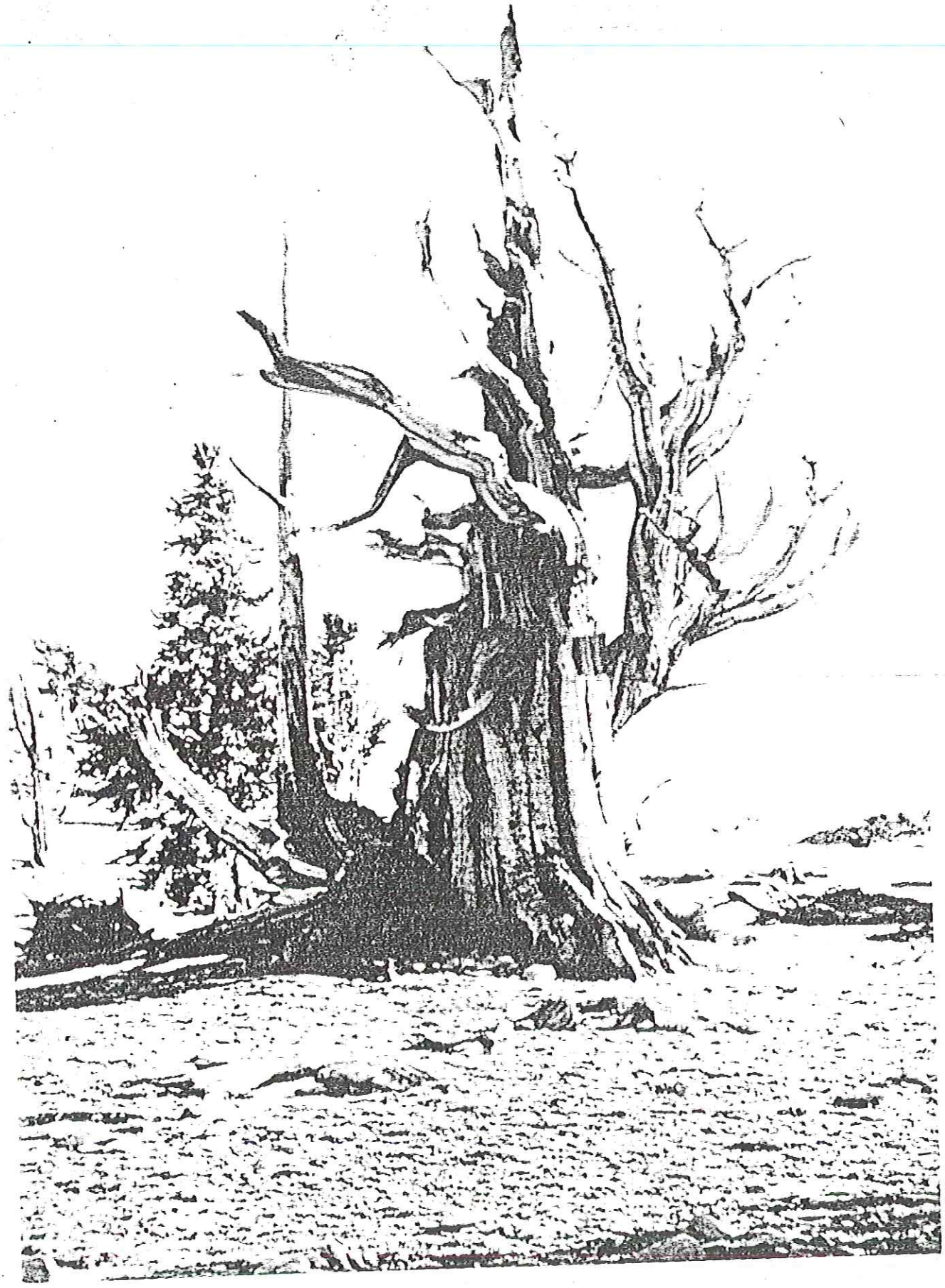

1. Earth's oldest inhabitant, the bristlecone pine. In the White Mountains of California these trees reach an age of 4,000 years.

Minze Stuiver – refined bristlecone pine ^{14}C calibration

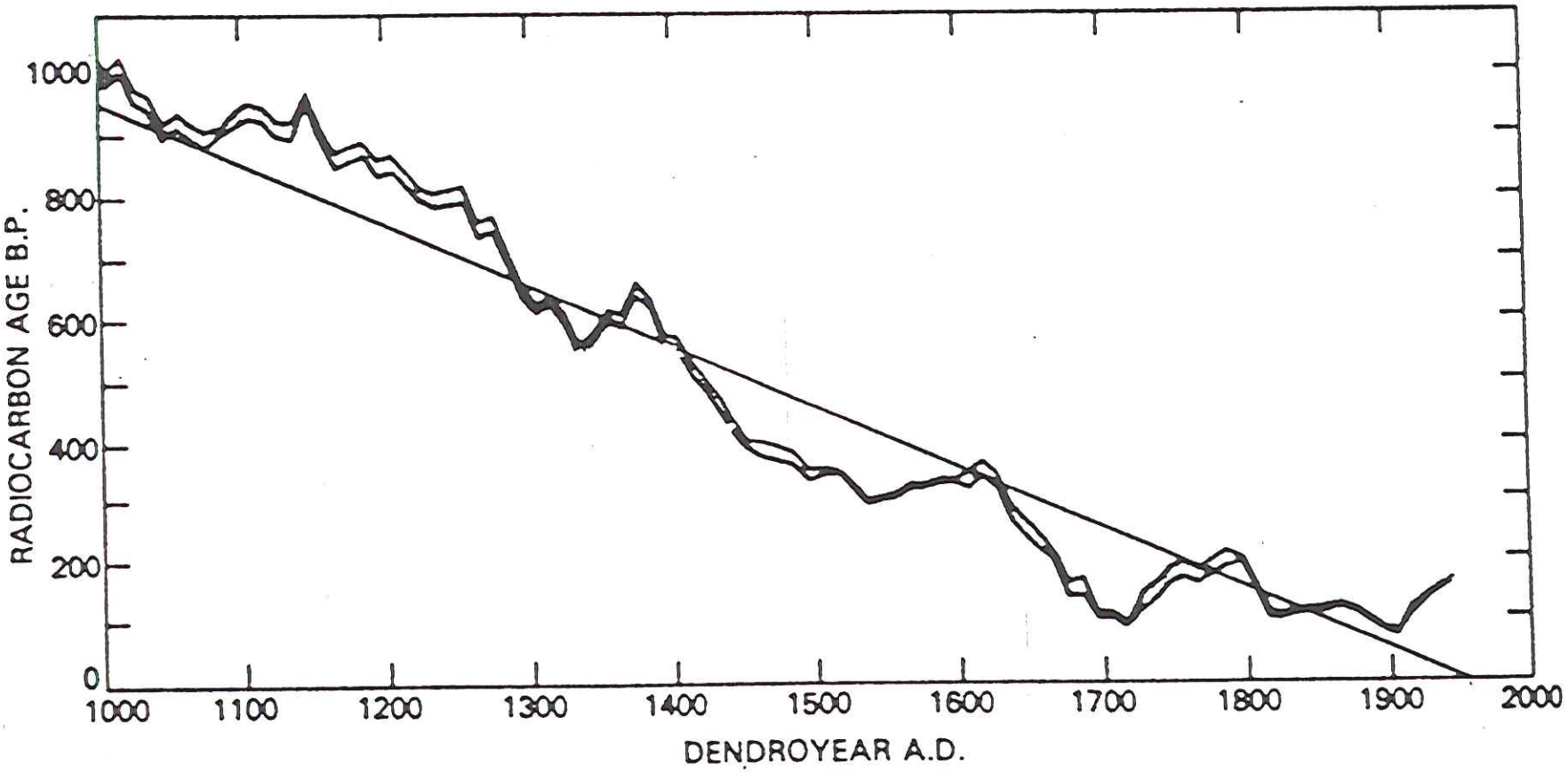

FIGURE 13.4 Carbon-14 age as a function of dendrochronological age for the past 1000 yr (from Stuiver, 1982). Note deviations from concordance line that have a 100-200-yr period.

last 1000 yrs only

^{14}C dating has had a profound impact on archaeology.

Any artifact containing organic carbon can be dated.

One of many examples — bronze age Europe — prior to advent of ^{14}C dating, it was felt that Stonehenge must have postdated and, in fact, been influenced by the Mycenaean culture of Greece — capable of building such edifices — lion gate, beehive tombs.

Mycenae — beginning ~ 1600 BC — based upon historical accounts of Agamemnon, etc. — e.g. Homer

Felt that Stonehenge no earlier than 1400 BC

But ^{14}C dating showed Stonehenge in fact ~ 2000 BC — prior to Mycenae

Forced a complete re-examination of the so-called Wessex culture bronze age

Before Civilization — Colin Renfrew — discusses this

12. The great stone rotunda at Stonehenge, built *c.* 2000 B.C. (Stonehenge IIIa).

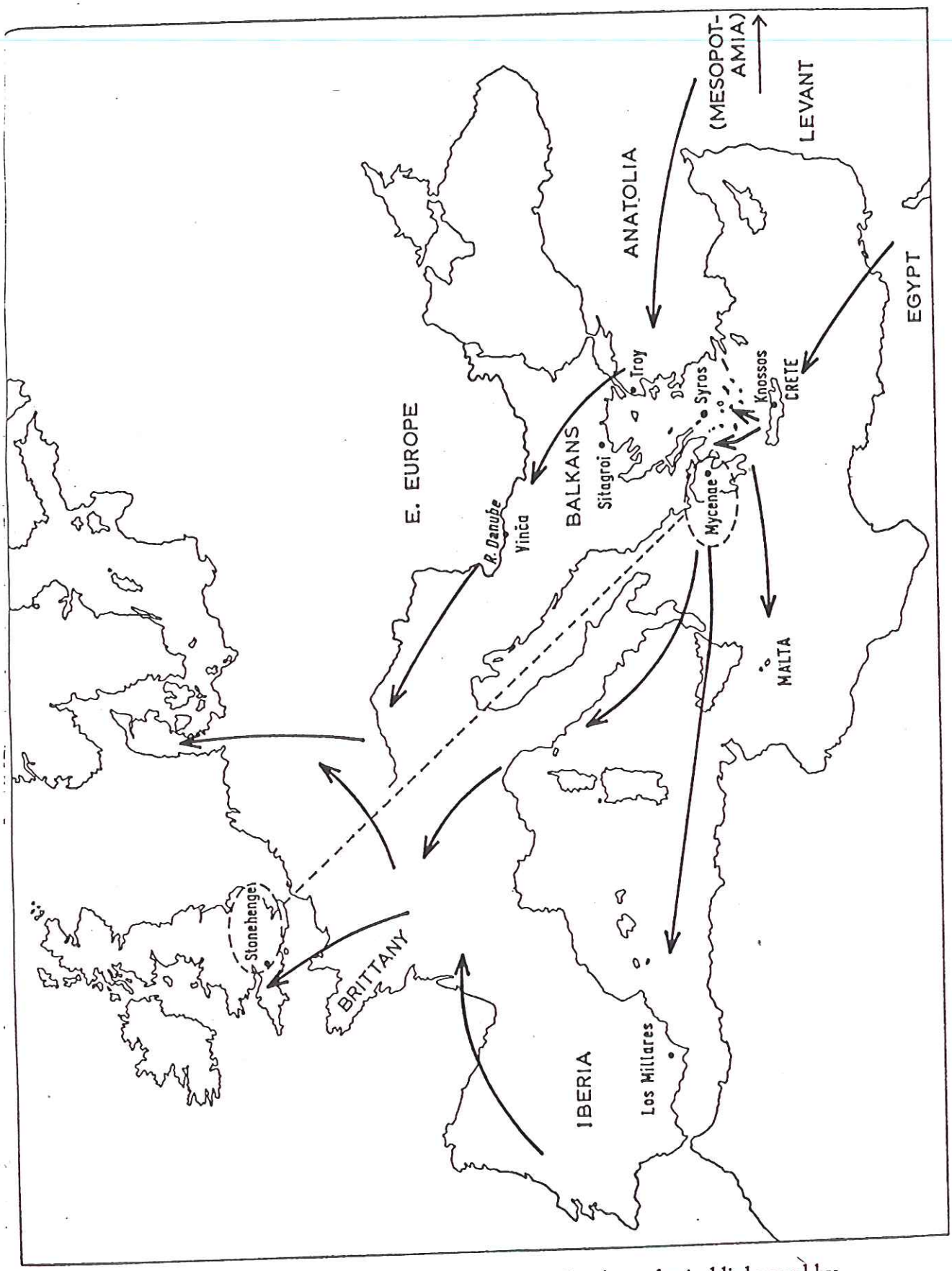

FIG. 6. Map of Europe with arrows indicating the chronological links used by Childe to date prehistoric cultures, by reference to the historical calendars of ancient Egypt and Mesopotamia.

Lion Gate at Mycenae

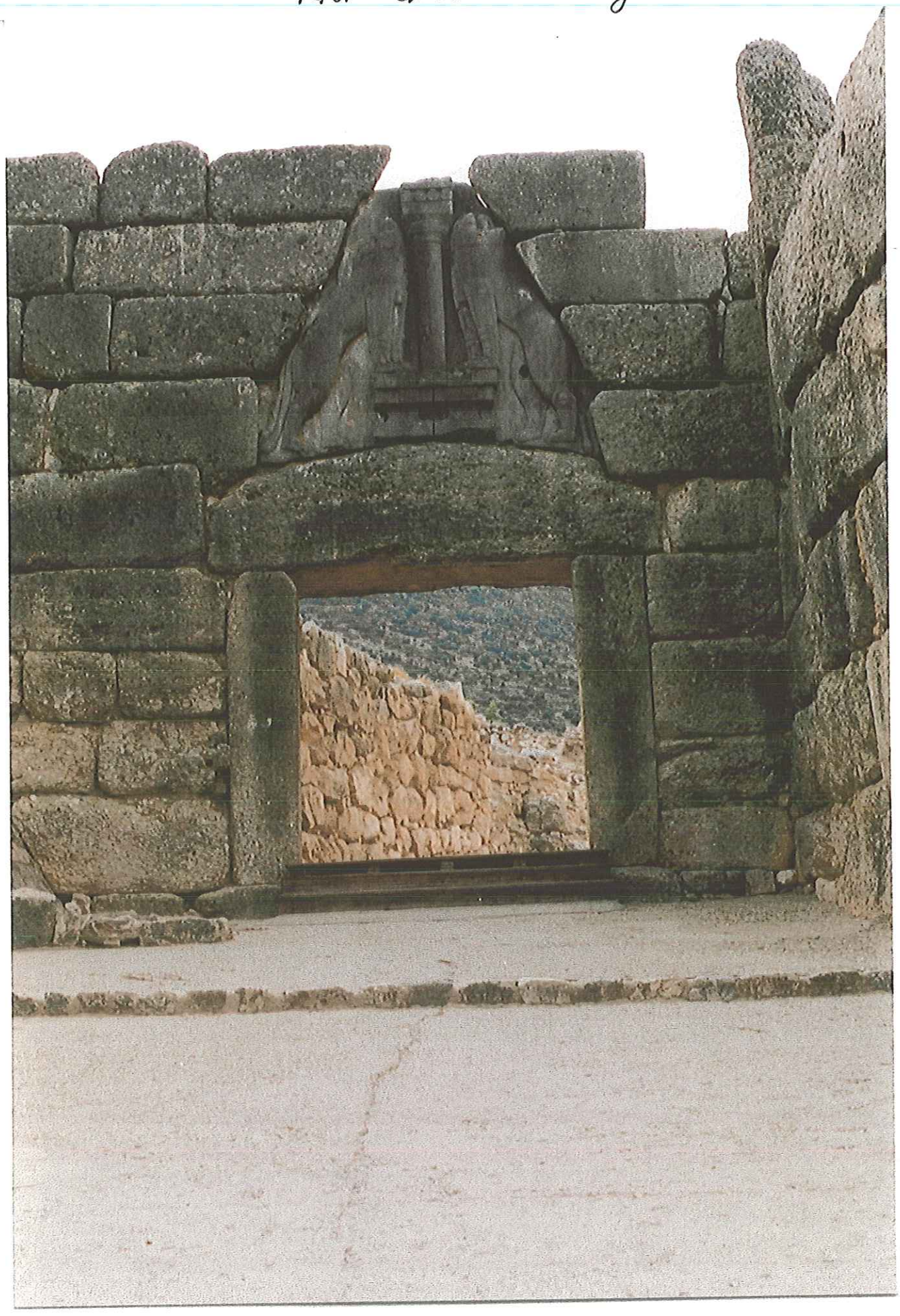

Childe's third major element in the chronological structure was of later date. He saw that the early bronze age of central and northern Europe, with its rich princely burials, possessed a number of exotic features not unlike those of the Mycenaean culture of Greece. At Mycenae the rich Shaft Graves, dated around 1600 B.C., had contained numerous swords, a wealth of gold, and quantities of amber beads which must have been imported from the Baltic area; and in north Europe, notably in the Wessex area of Britain, the princely burials in dagger graves were sometimes furnished with gold objects and frequently contained amber beads. Indeed the burials of south Britain – the so-called Wessex culture – seemed to furnish a number of indications, such as the faience beads (described in Chapter 5), of direct contact with the Mycenaean world. Childe concluded that the early bronze age of Europe was dependent on, and therefore later than, the Mycenaean civilization. As he wrote in his last book, published in 1958:

> While a distinctive bronze industry was being established around the Aegean, a neolithic economy still persisted north of the Balkans, the Alps and the Pyrenees. The Early Aegean Age corresponds in time to parts at least of Middle or Late Neolithic in Temperate Europe. But at least during the latter period, ripples generated by the Urban Revolution were already disturbing the self-sufficiency of the peasant communities. At the same time 'political events' – migrations and conquests – were preparing the sociological foundations for a Bronze Age economy.[20]

On this basis, the early bronze age Wessex culture was set around 1400 B.C., well after the beginning of Mycenaean civilization around 1600 B.C. The whole question of the British early bronze age, and of Stonehenge (which is generally set in the same period), is discussed in Chapter 11; its particular interest here is the way it was used to help build up a coherent structure for the dating of Europe.

European chronology, and hence the whole sequence of events that prehistorians reconstructed, was built on these three crucial links. Spain and the Balkans were both dated on the basis of supposed contacts with the Aegean. France and central Europe could then be tied in with their respective neighbours to the south. So, by a series of chronological steps, the whole of Europe was brought into contact with the world of the

A radiocarbon date from the Helmsdorf barrow in north Germany, for instance, which should be broadly contemporary with at least part of the Wessex culture, can be set around 1900 B.C. after calibration. And other similar dates are now beginning to form a pattern.

Using such evidence, which is admittedly indirect, I suggested in 1968, in a paper called 'Wessex without Mycenae', that the duration of the Wessex culture might have been from about 2100 to 1700 B.C. in calendar years. Radiocarbon dates from two dagger graves, quoted in Chapter 5, indicate now that rich burials of this kind must have continued until at least 1500 B.C. But they do not conflict with the early date suggested for the first of the Wessex dagger graves. We do not yet have enough dates from Wessex to give a final verdict on this question – and Christopher Hawkes, a leading scholar of the early Wessex bronze age, has argued with vigour against the early dating. But whatever the date, my own view is that the Mycenaean contacts with Wessex, if they existed at all, were of very marginal importance.

In any case, the radiocarbon dates which we have for Stonehenge now suggest that it was completed before Mycenaean times. Using the uncalibrated radiocarbon dates, Atkinson came to the conclusion that the main structure, Stonehenge III, was erected in the seventeenth century b.c., in radiocarbon years. If we accept this, using Suess's calibration curve, we would reach a date of between 2100 and 1900 B.C. in calendar years. Because of these early dates, some scholars, including Christopher Hawkes, now feel that Stonehenge III was actually built before the time of the Wessex culture. But of course, if the early Wessex dating is accepted, the construction date of 2100 to 1900 B.C. is in any case within the Wessex culture time-span.

The effect of the tree-ring calibration of radiocarbon upon the Wessex culture and Stonehenge is not so dramatic as it was for the megalithic tombs, or for the copper age in south-east Europe. This is partly because we have as yet rather few relevant radiocarbon dates. But it is also because the Wessex culture was rather later than these other cases. So that whereas a radiocarbon date of 2500 b.c. will be set 800 years earlier in calendar years, one of 1500 b.c. moves back by only two or three centuries (see Fig. 14). I believe, however, that the time shift is sufficiently drastic to make us look at Stonehenge and the wealth of the Wessex graves in their own right. For even if there were trading links with Mycenae – and the

A second application — determination of earthquake recurrence intervals

Kerry Sieh (Caltech) — paleoseismology

Extrapolation of the quake record beyond the historical (felt & recorded by people) past

Magnitude $M > 8$

Fort Tejon quake

Example — 1857 ruptured a 300 km long segment of San Andreas fault

when will the next large earthquake occur on this segment of the fault. Has been quiescent since 1857

this is the Big One LA is awaiting

1857 — only 8 years after SF gold rush this portion of Calif sparsely populated

[redacted]

Show picture of fault in Carrizo Plain

Technique developed by Sieh — trenching

Show color photo of trench

look for small features in sidewall indicative of past motions

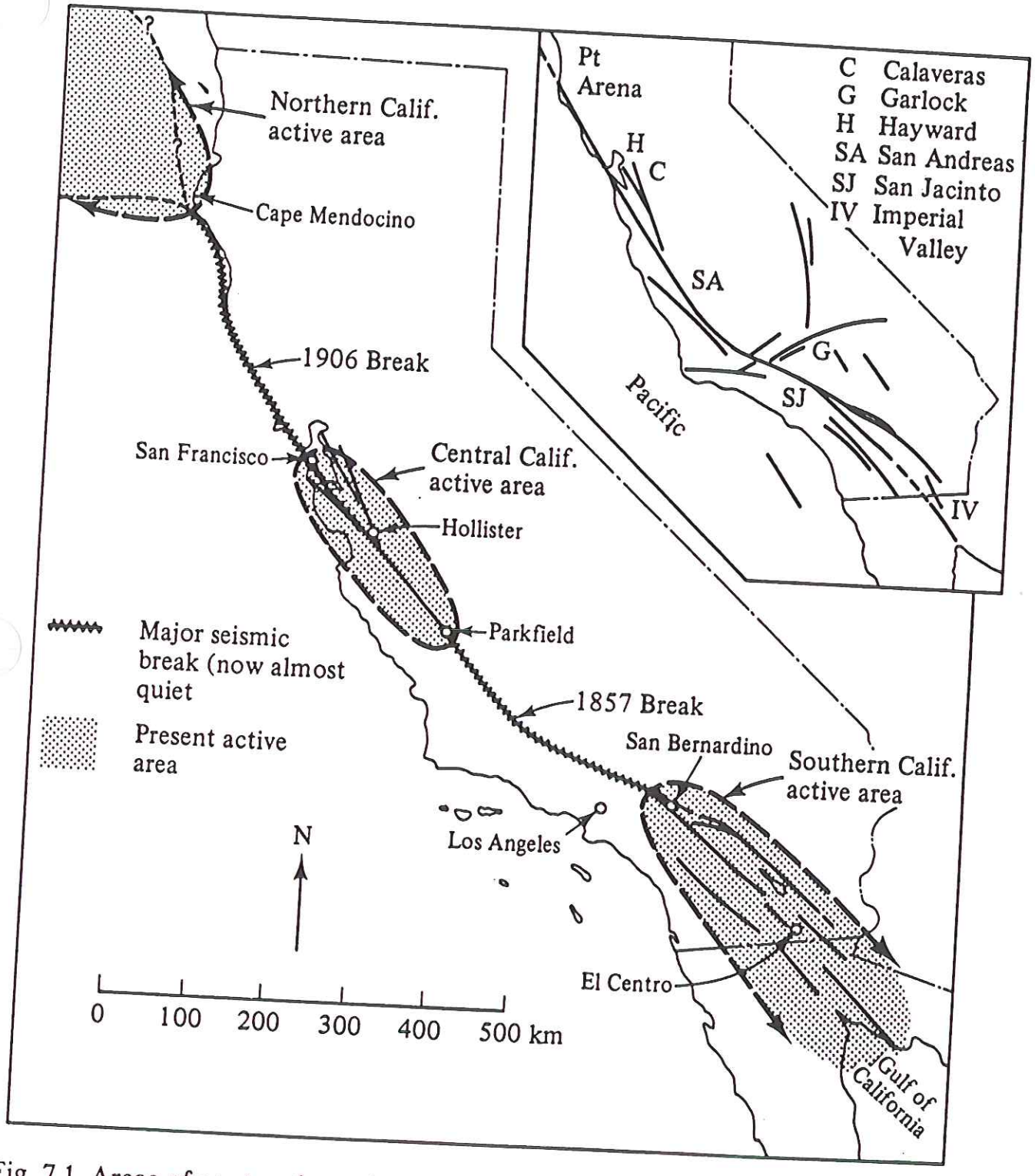

Fig. 7.1. Areas of contrasting seismic behaviour along the San Andreas fault zone in California. (After Allen, 1968.)

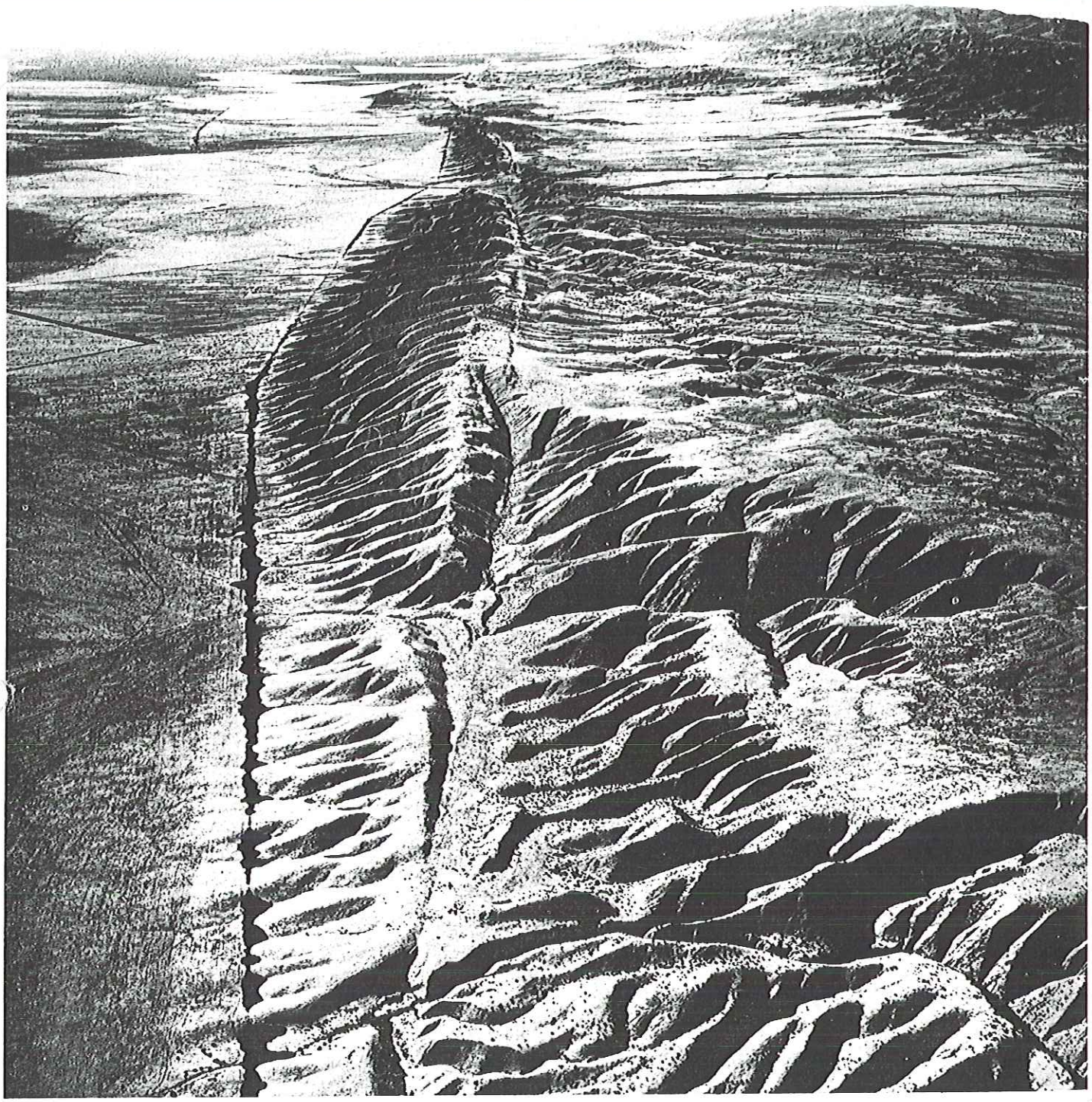

Fig. 8-58 shows examples of types of features

(a) Most slip is in and out of page but also slight up-and-down motions

Can offset beds

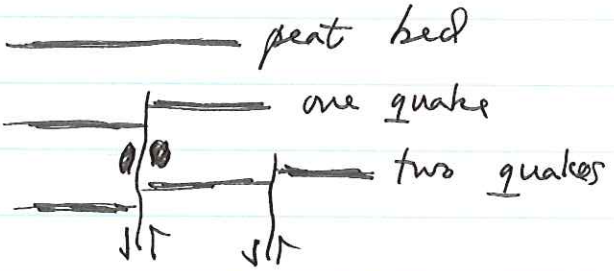

or make small alluvial or "landslide" wedges

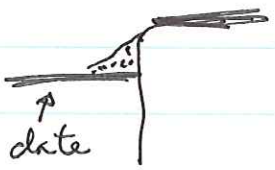

One looks for small pieces of charcoal — from forest fires — or, frequently, peat beds to ^{14}C date

Color figure shows a second type of feature that can ~~[illegible]~~ be found in ~~[illegible]~~ trenches — a sandblow

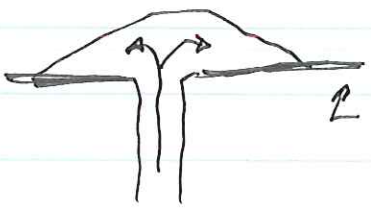

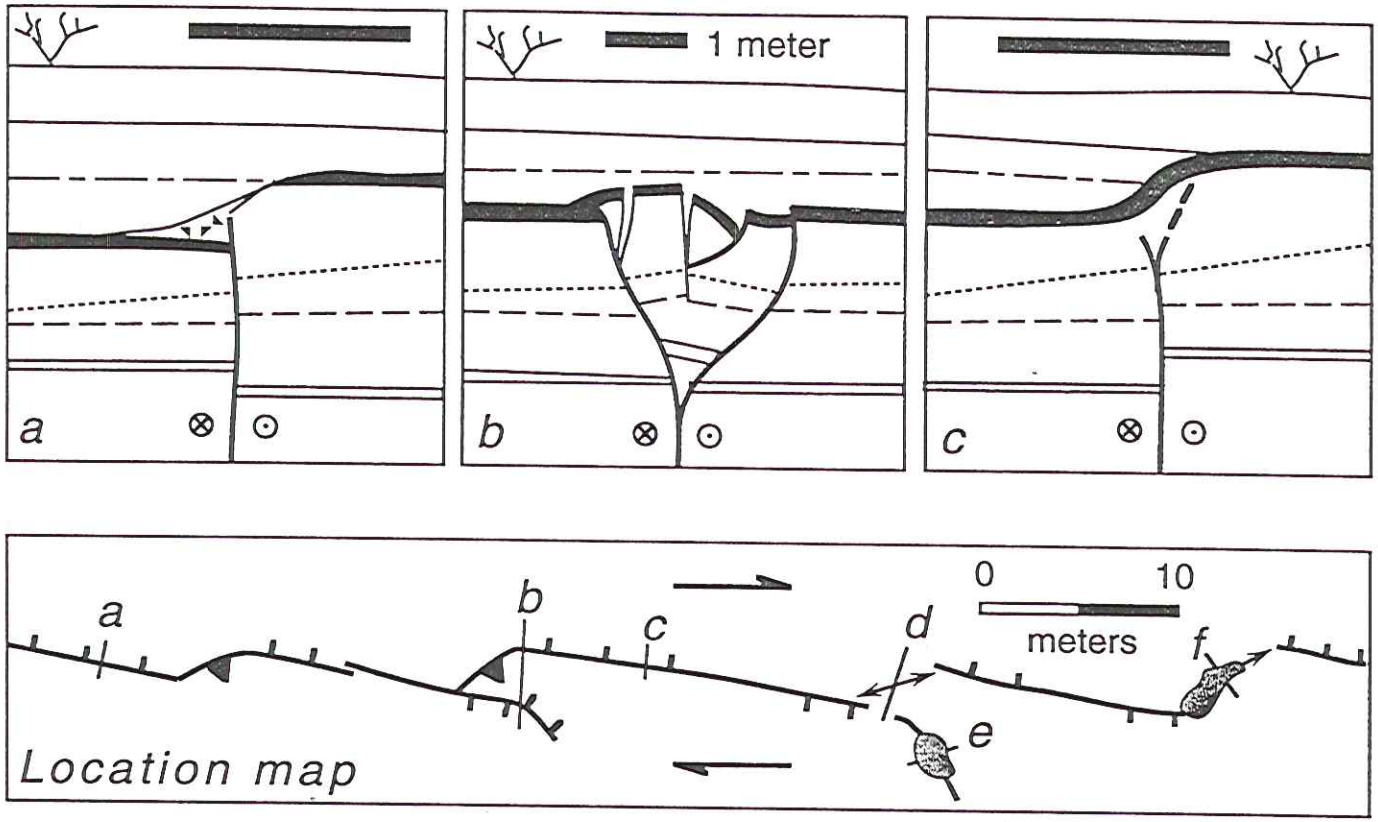

Figure 8–58. These idealized cross sections across strike-slip faults show various kinds of evidence for paleoseismic events. Top of solid black bed is the event horizon. Shaded horizontal bars are 1 meter long. Lines with arrows on location map indicate crests of anticlinal folds. Mismatches of strata across some of the faults is an indication of strike-slip motion.

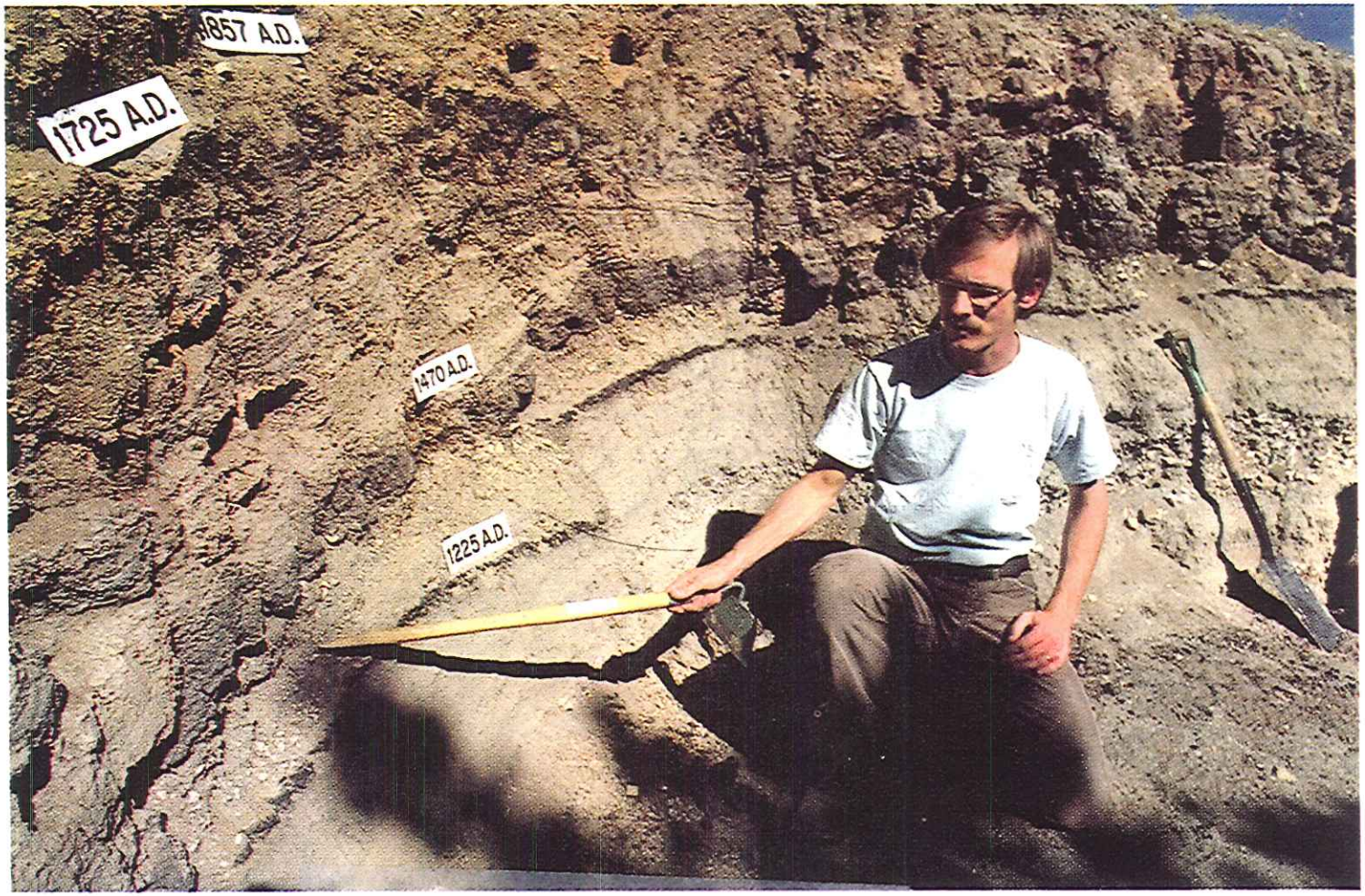
1857 A.D.
1725 A.D.
1470 A.D.
1225 A.D.

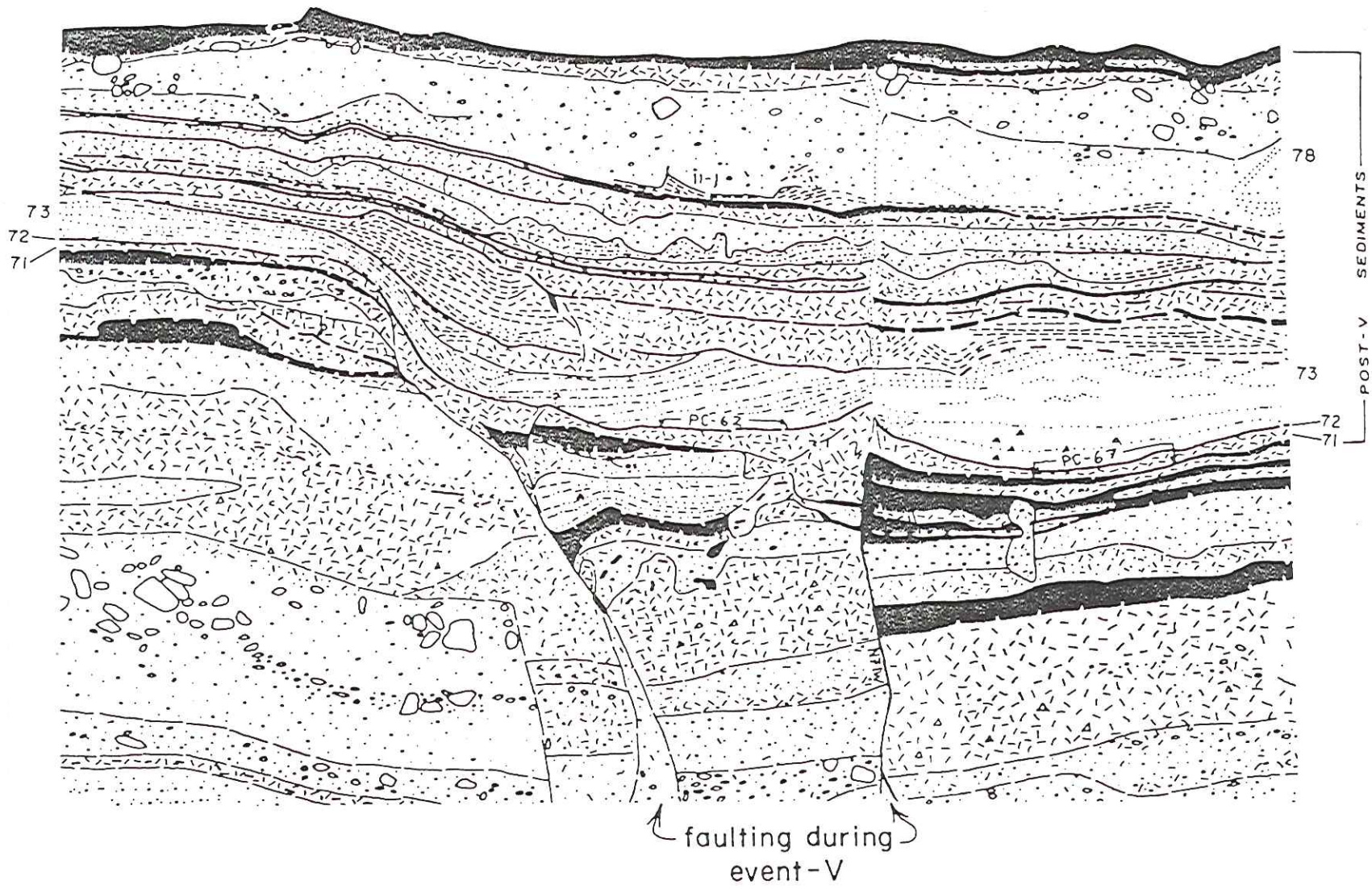

Figure 8–59. Examples of cross-sectional exposures of paleoseismic events in strike-slip fault zones. (a) Fault breaking marsh peats, aeolian silts, and fluvial sands and gravels is associated with oblique dextral slip on the San Andreas fault in about A.D. 1480. One inch equals one-half meter. From Sieh (1978a).

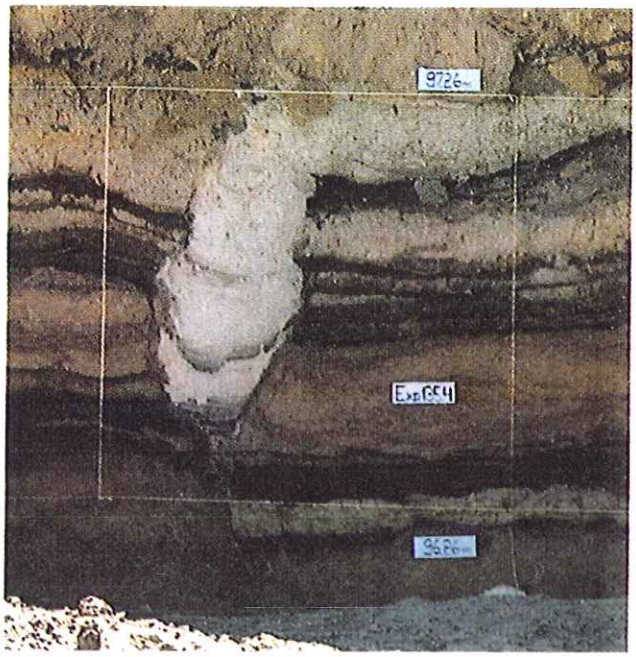

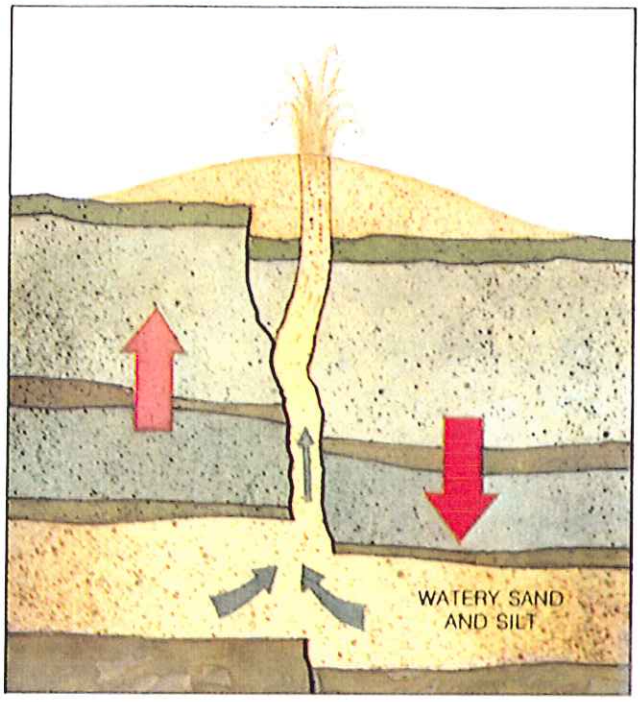

Remnants of a sandblow—a spouting of sand and water caused by moderate to severe earthquakes—can be seen in the photograph of a cross section of an old California stream bed that was rocked by a quake around 1700. Sandblows occur, as illustrated in the drawing at bottom, when a layer of subsoil takes on liquid characteristics during tremors. Pressure drives the watery sand and silt up through a fissure, leaving a mound of sediment on the surface that geologists can use to identify and date the earthquake.

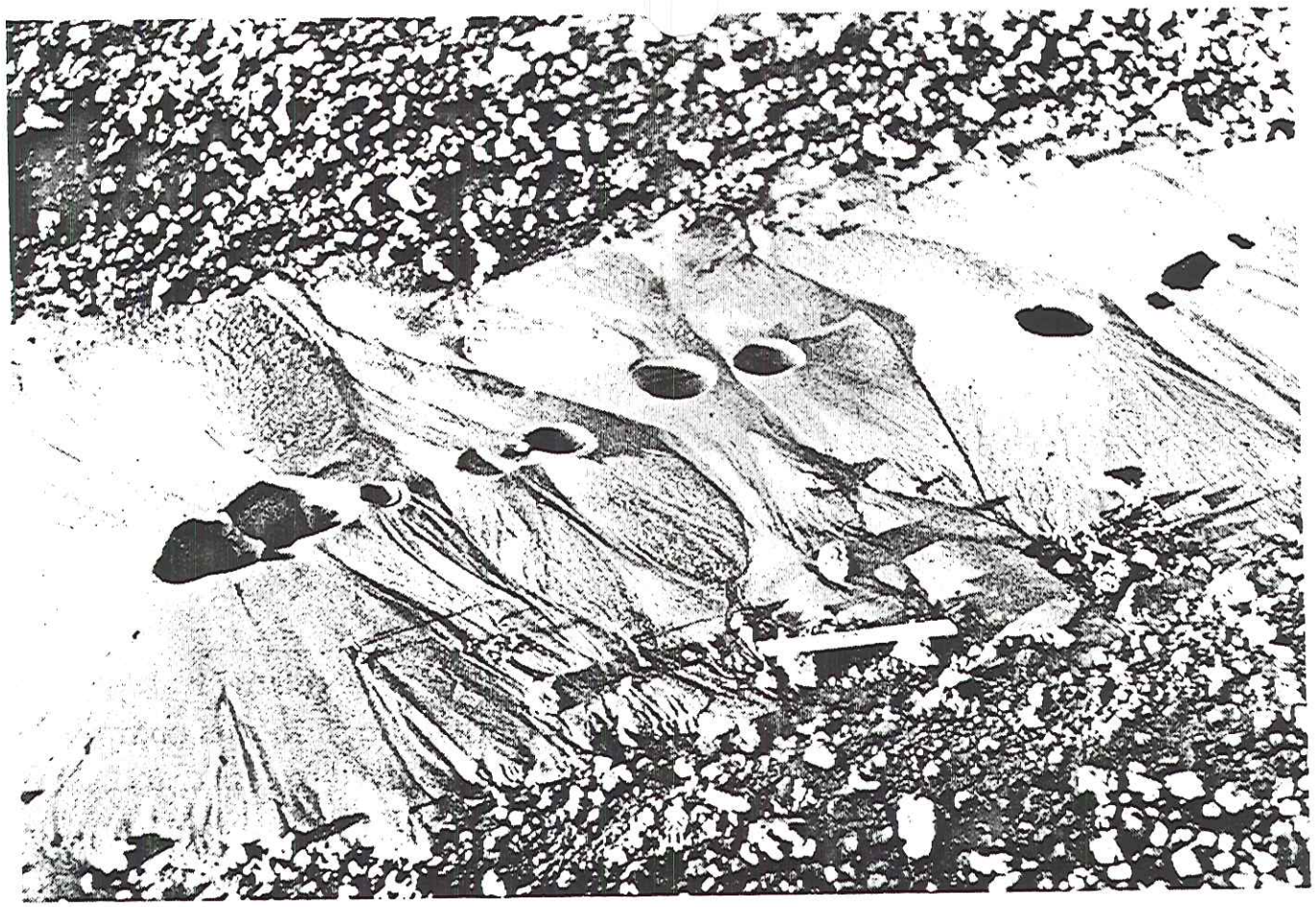

Figure 12–6. Sand blows from the M6.6 Imperial Valley, California, earthquake of 15 October 1979, in a field north of Heber Dunes. The circular vents are aligned along a fracture in a lateral spread at Heber Road. Scale is 22 cm long. Photo taken 16 October by Kerry Sieh.

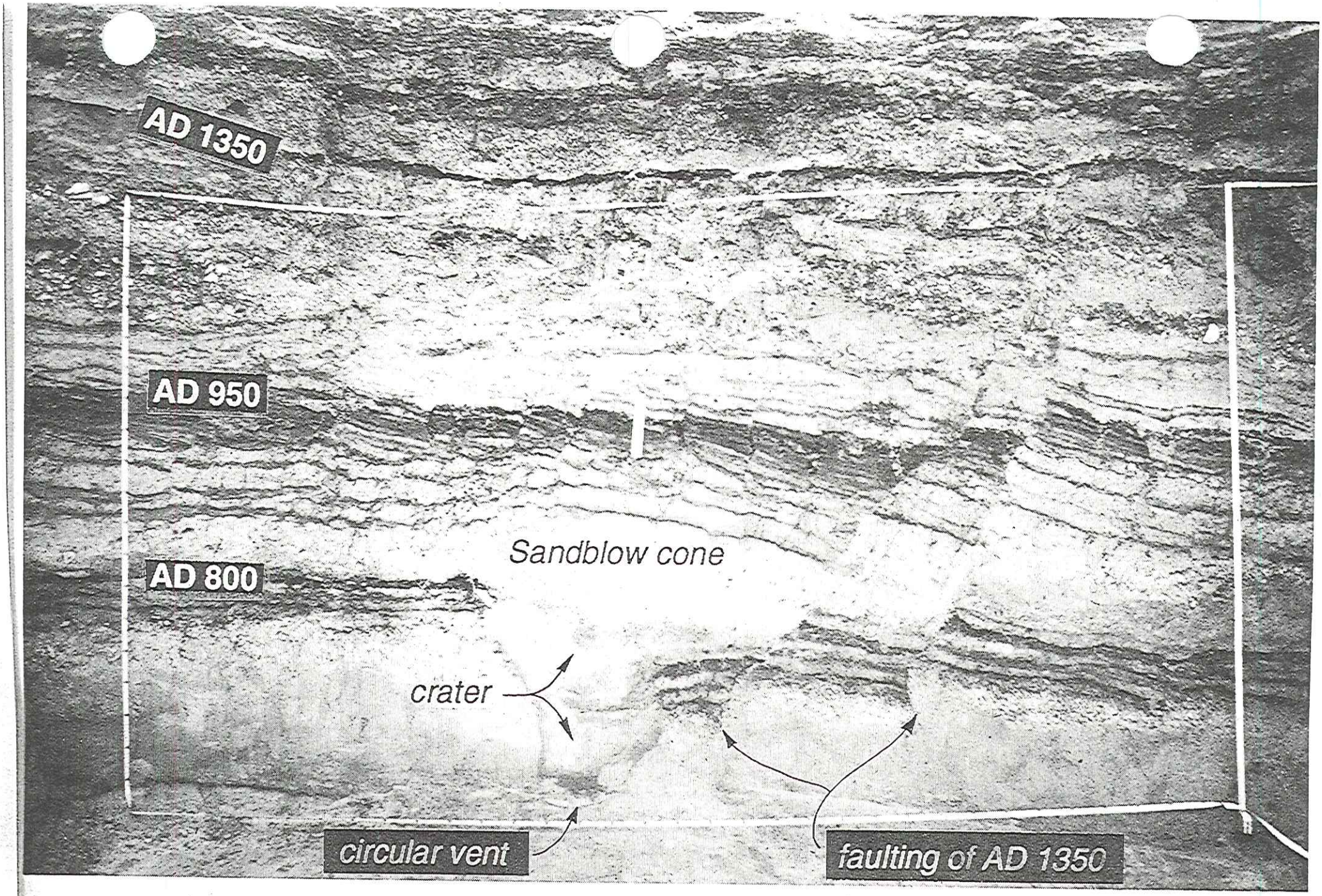

Figure 8–59. (b) Sandblow associated with dip-slip faulting in San Andreas fault zone, about A.D. 800.

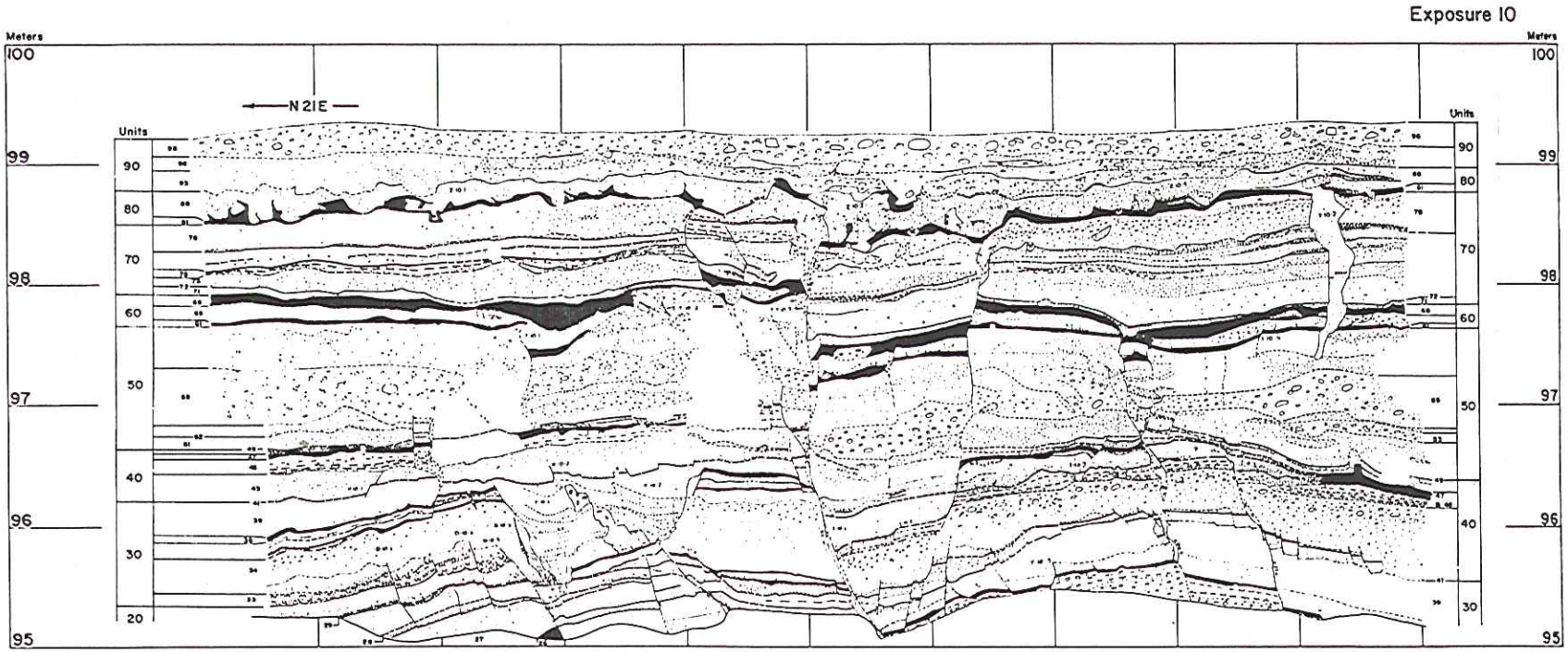

Figure 8–60. Map of trench wall shows evidence for eight earthquakes on San Andreas fault between about A.D. 750 and 1857. Grid spacing is one meter. For large-scale reproduction, see Sieh (1978a).

Fig. 18.60 shows evidence for eight earthquakes in a single 5 m deep x 15 m long trench at Pallett Creek

Fig. 6 shows dates for ten quakes at Pallett Creek

2 = 1857 'quake

The mean recurrence interval is

~~140~~ 130 years on Mohave segment of SAF

Time since 1857 — more than 140 yrs

Note, however, the evidence for clustering.

Fig. 8-65 shows the history of ruptures at other points along the SAF up to Parkfield in N. Calif.

On the basis of this "woefully incomplete" record the Working Group on California Earthquake Probabilities has assigned a 30% probability to an M=8 'quake on Mojave segment (LA's big one) ~~[illegible]~~ in next 20 years — before 2018

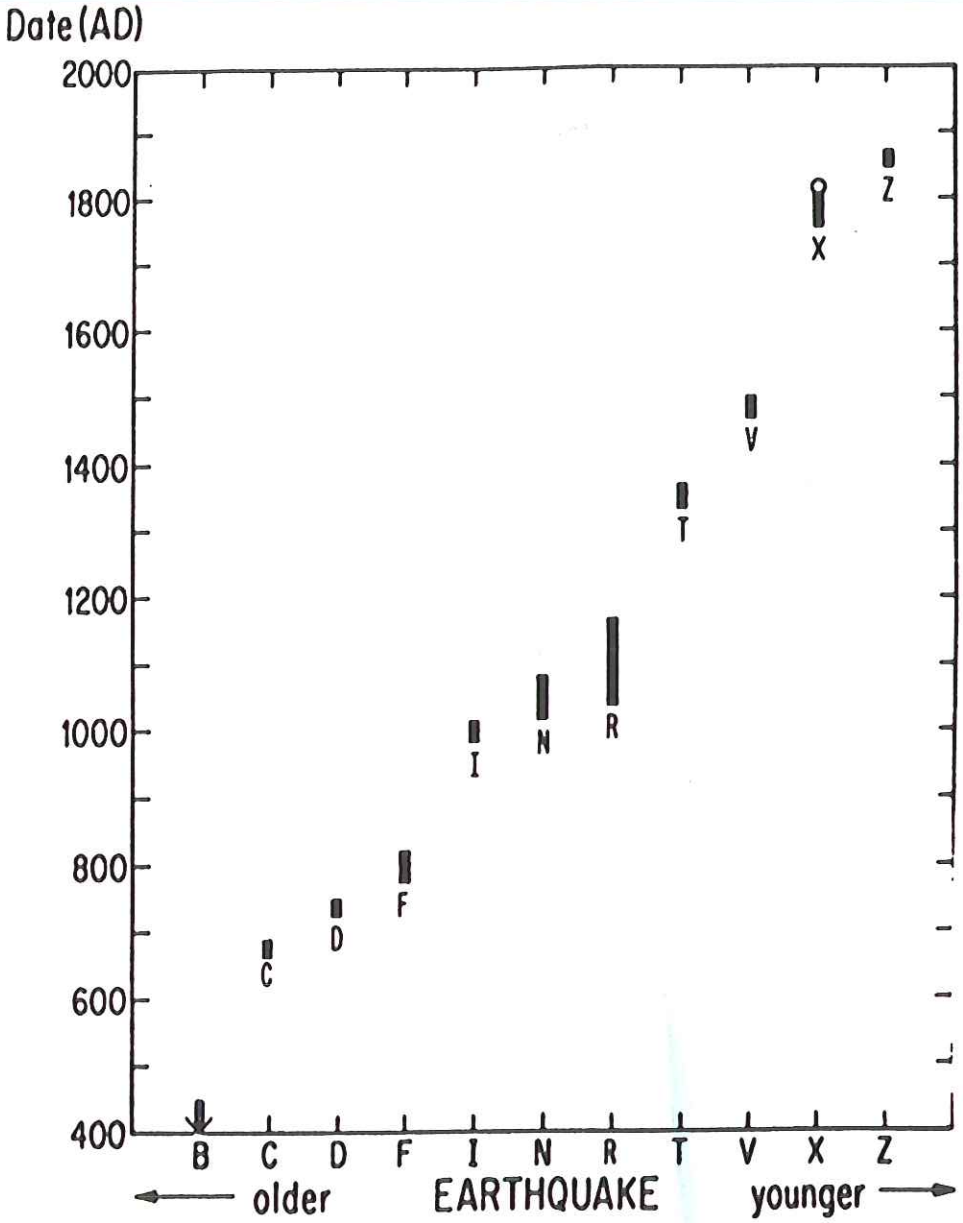

FIGURE 11.47 Dates of the inferred last 10 earthquakes on a section of the southern San Andreas fault at Pallet Creek. The dates were determined from organic materials trapped along disturbed strata. (From Sieh *et al.*, *J. Geophys. Res.* **94**, 603–624, 1989; © copyright by the American Geophysical Union.)

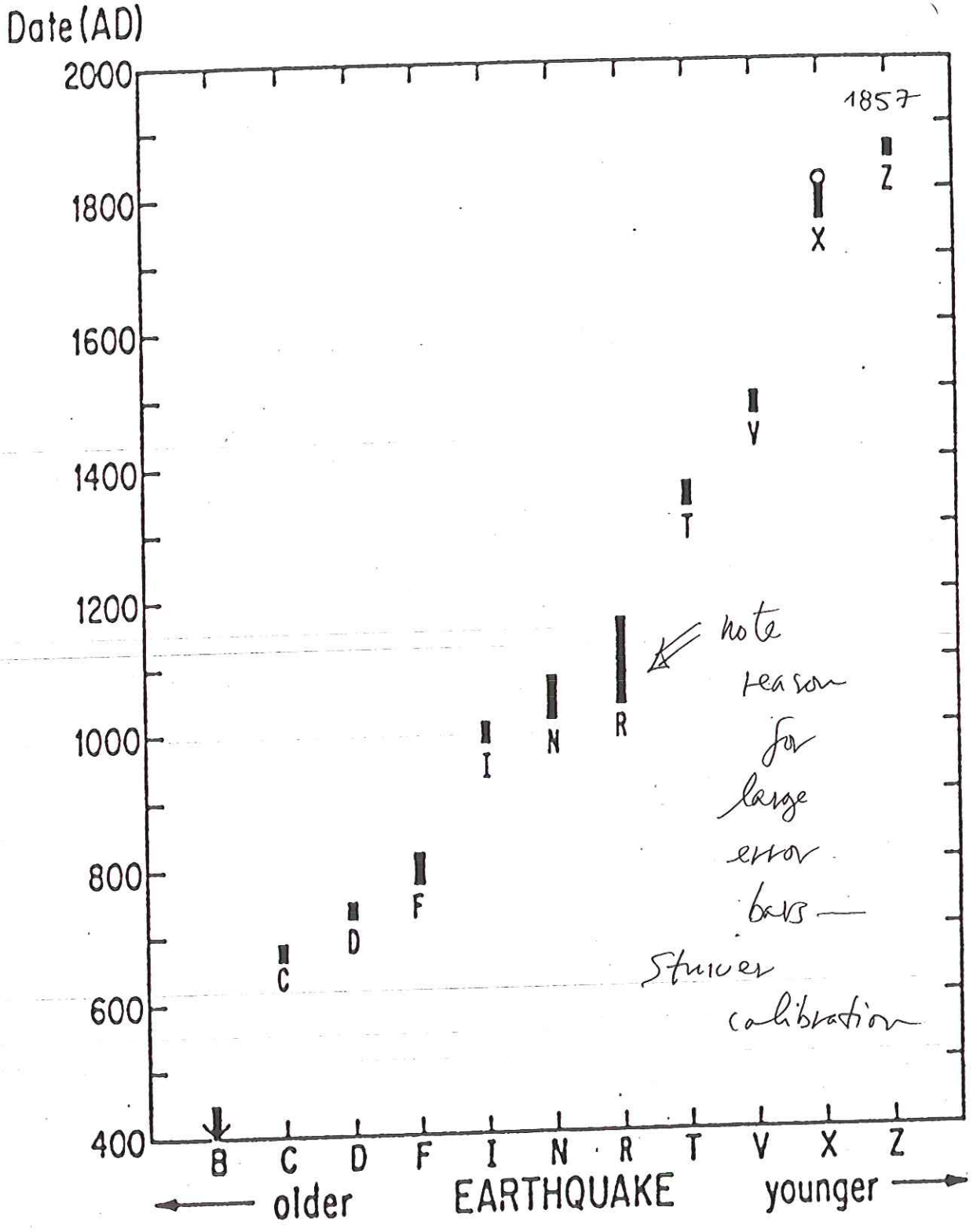

Fig. 6. New estimates of the dates for earthquakes recorded in the sediments at Pallett Creek. Bars give 95% confidence intervals. Open circle on bar of event X indicates preferred date of A.D. 1812.

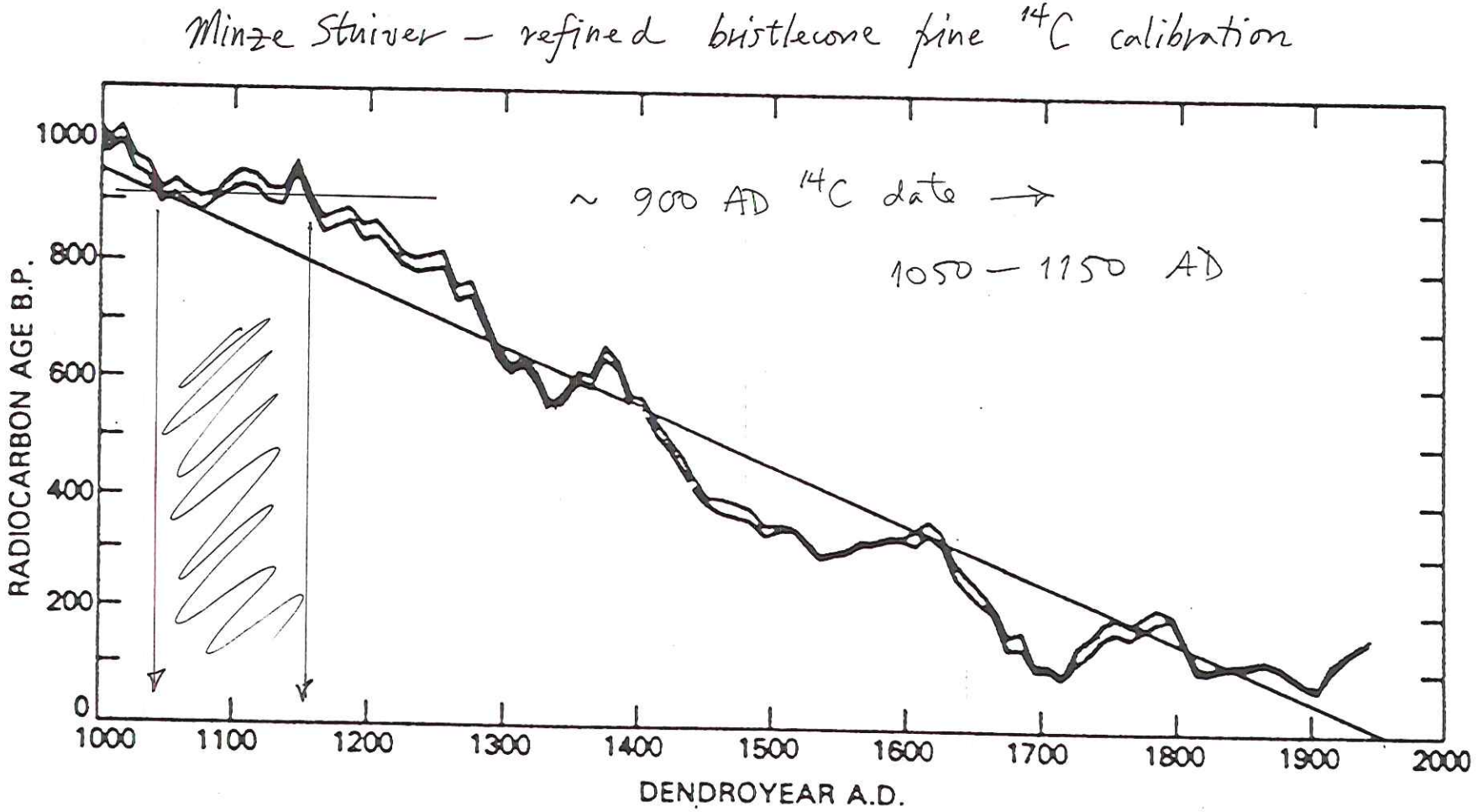

FIGURE 13.4 Carbon-14 age as a function of dendrochronological age for the past 1000 yr (from Stuiver, 1982). Note deviations from concordance line that have a 100-200-yr period.

last 1000 yrs only

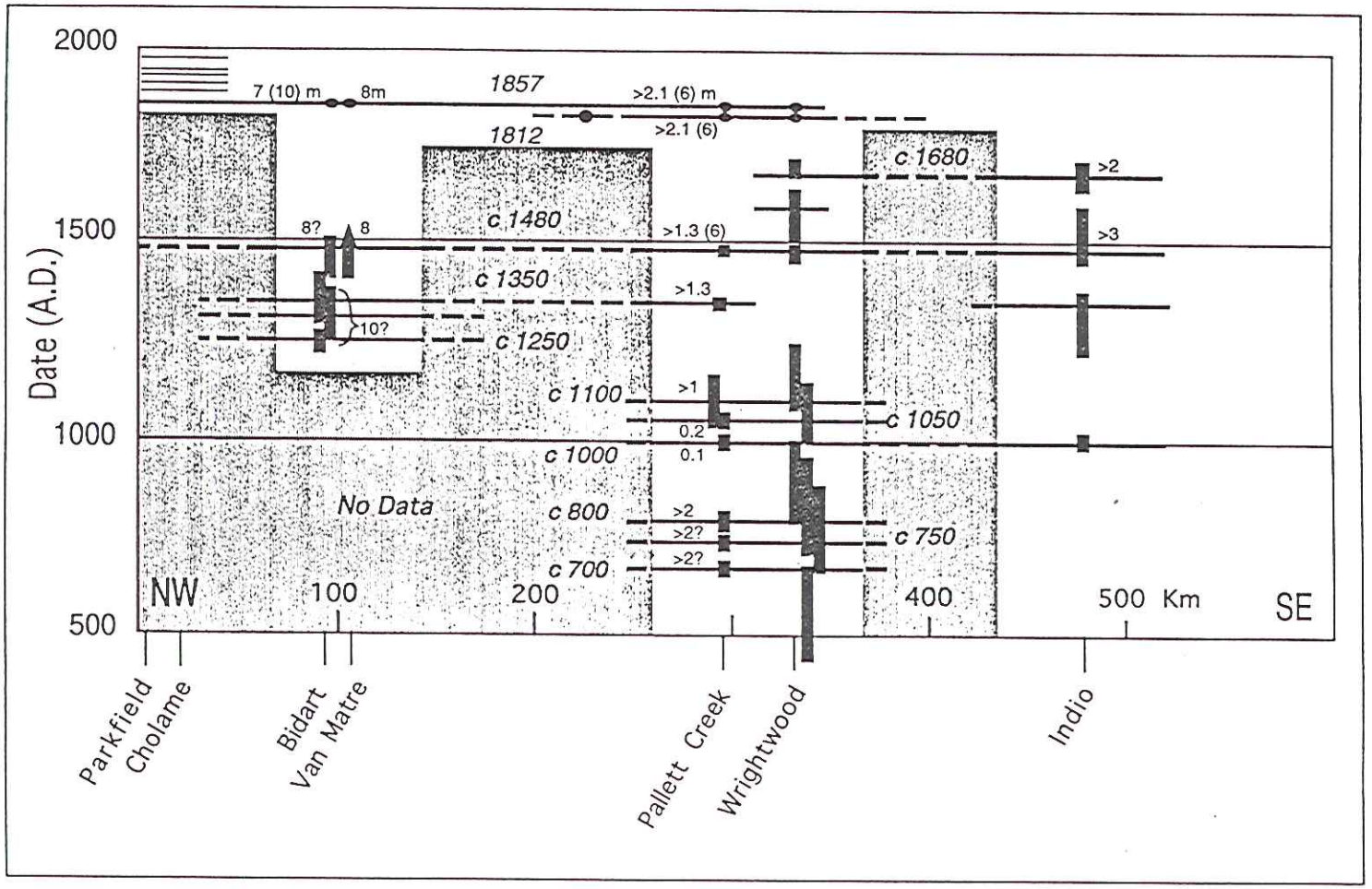

Figure 8–65. This history of large ruptures along the San Andreas fault is based upon data from several paleoseismic sites. Thick horizontal lines represent rupture lengths, based upon proposed correlations between sites. Dextral offsets are indicated (in meters) where available. Offsets in parentheses represent broad-aperture values, whereas others represent offsets measured in 3D excavations only within the fault zone. Values queried where more speculative. Though woefully incomplete, the currently available record demonstrates the clustered nature of earthquake occurrence along the fault and the inappropriateness of the characteristic- or uniform-earthquake model for the San Andreas fault. Modified from Grant and Sieh (1994), with additions from Sieh (1984), Salyards et al. (1992) and other sources.

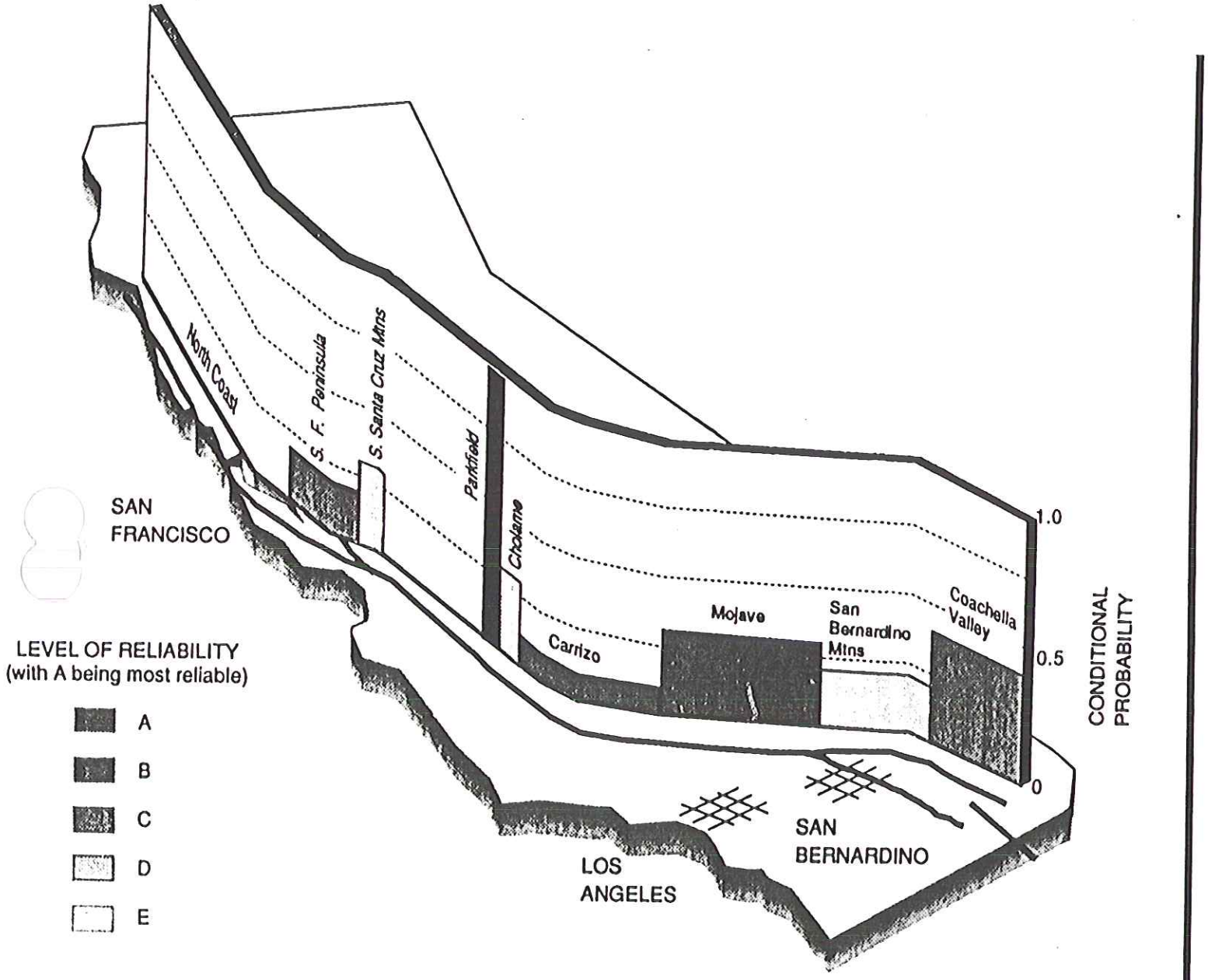

FIGURE 11.B3.2 The conditional probability of major earthquakes along different segments of the San Andreas fault. The probability illustrated is for the time interval 1988–2018. (From Agnew *et al.*, 1988).